

## SUPPORTING INFORMATION

### Achieving red-light anticancer photodynamic therapy under hypoxia using Ir(III)-COUPY conjugates

Enrique Ortega-Forte <sup>a,c</sup>, Anna Rovira <sup>b</sup>, Pezhman Ashoo <sup>a</sup>, Eduardo Izquierdo-García <sup>b</sup>, Cormac Hally <sup>c</sup>, Diego Abad-Montero <sup>b</sup>, Mireia Jordà-Redondo <sup>c</sup>, Gloria Vigueras <sup>a</sup>, Alba Deyà <sup>d</sup>, José Luis Hernández <sup>d</sup>, Jorge Galino <sup>d</sup>, Manel Bosch <sup>e</sup>, Marta E. Alberto, <sup>f</sup> Antonio Francés-Monerris, <sup>g</sup> Santi Nonell <sup>c</sup>, José Ruiz <sup>\*a</sup>, Vicente Marchán <sup>\*b</sup>

<sup>a</sup> Departamento de Química Inorgánica, Universidad de Murcia, Biomedical Research Institute of Murcia (IMIB-Arrixaca), E-30100 Murcia, Spain. E-mail: jruiz@um.es.

<sup>b</sup> Departament de Química Inorgànica i Orgànica, Secció de Química Orgànica, Universitat de Barcelona (UB), Institut de Biomedicina de la Universitat de Barcelona (IBUB), Martí i Franquès 1-11, E-08028 Barcelona, Spain. E-mail: vmarchan@ub.edu.

<sup>c</sup> Institut Químic de Sarrià, Universitat Ramon Llull, Vía Augusta 390, E-08017 Barcelona, Spain.

<sup>d</sup> Health and Biomedicine Department, Leitat Technological Center, Carrer de la Innovació 2, E-08225 Terrassa, Spain.

<sup>e</sup> Unitat de Microscòpia Òptica Avançada, Centres Científics i Tecnològics, Universitat de Barcelona, Av. Diagonal 643, E-08028 Barcelona, Spain.

<sup>f</sup> Dipartimento di Chimica e Tecnologie Chimiche, Università della Calabria, Arcavacata di Rende I-87036, Italy

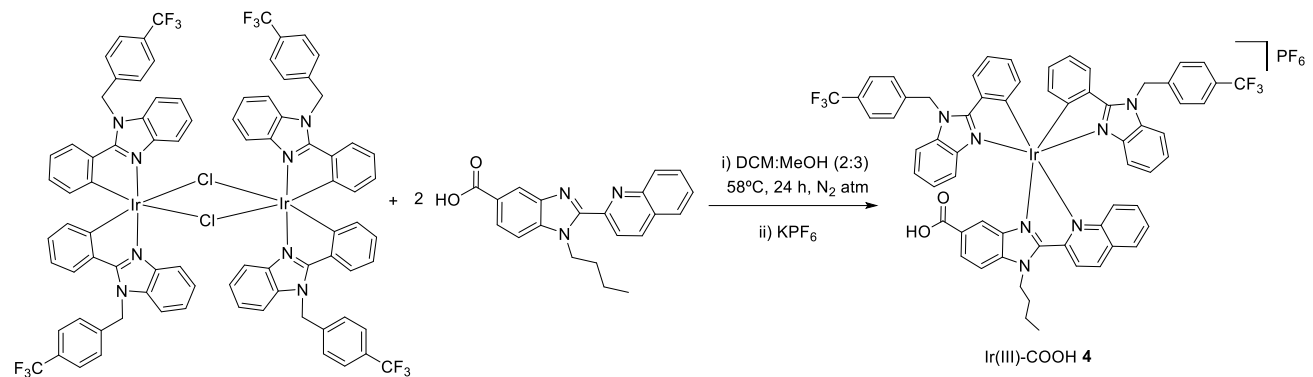
<sup>g</sup> Institut de Ciència Molecular, Universitat de València, P.O. Box 22085, València 46071, Spain

## **Table of contents**

<b>1.- Synthesis and characterization of Ir(III)-COUPY conjugate 3c</b>	S3
Ir(III)-complex <b>4</b> (Ir-COOH)	
Ir(III)-COUPY conjugate <b>3c</b>	
<b>2.- Photophysical characterization of the compounds</b>	S8
<b>3.- Photochemical characterization of the compounds</b>	S12
<b>4.- Dark and light stability of Ir(III)-COUPY conjugates in biological medium</b>	S17
<b>5.- Fluorescence imaging by confocal microscopy and accumulation studies by ICP-MS</b>	S25
<b>6.- Photobiological evaluation</b>	S28
<b>7. Cartesian Coordinates of the Ir(III)-COUPY conjugate 3c</b>	S41

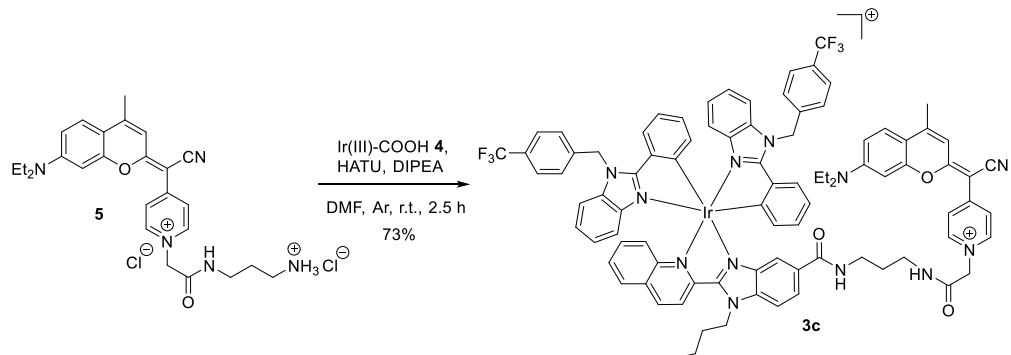
## 1.- Synthesis and characterization of Ir(III)-COUPY conjugate 3c

*Ir(III)-complex 4 (Ir-COOH).*



**Scheme S1.** Synthesis of Ir(III) complex **4**.

*Ir(III)-COUPY conjugate 3c.*



**Scheme S1.** Synthesis of Ir(III)-COUPY conjugate **3c**.

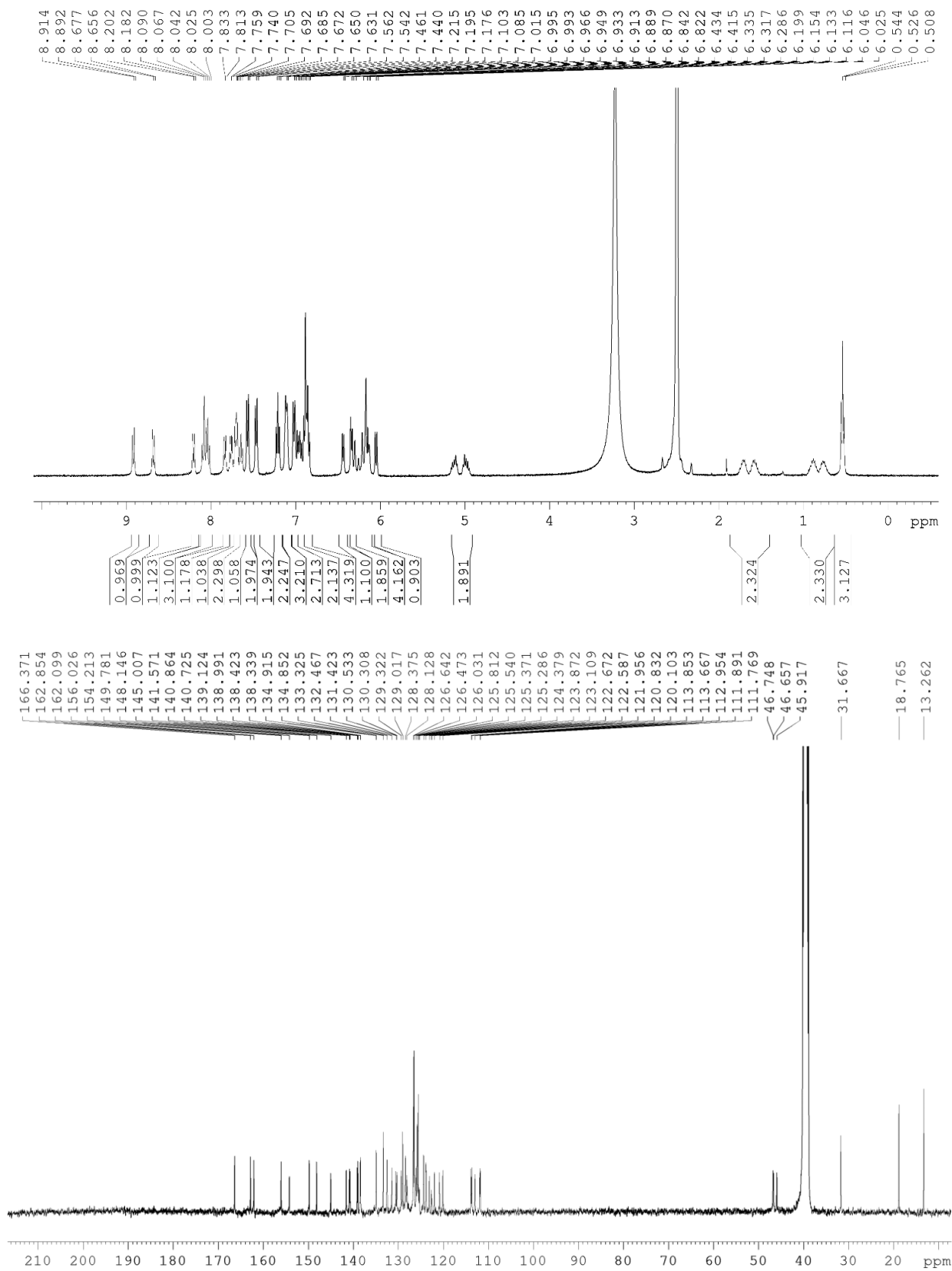


**Figure S1.**  $^1\text{H}$  and  $^{13}\text{C}$  NMR spectra of Ir complex **4** in  $\text{DMSO}-d_6$ .

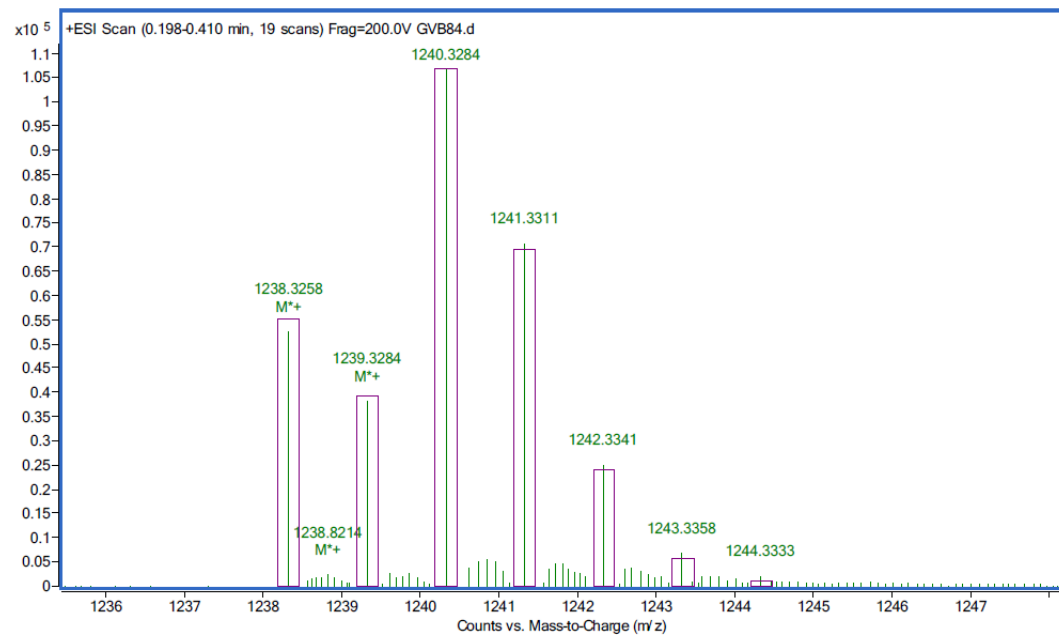
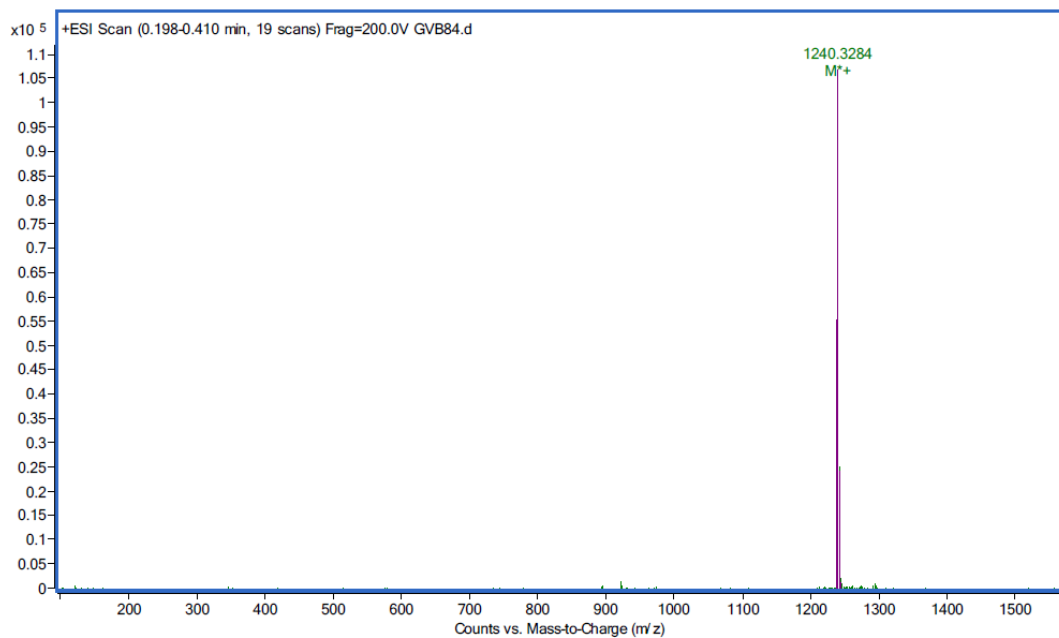


**Figure S2.** HR ESI-MS spectrum of Ir(III) complex 4.

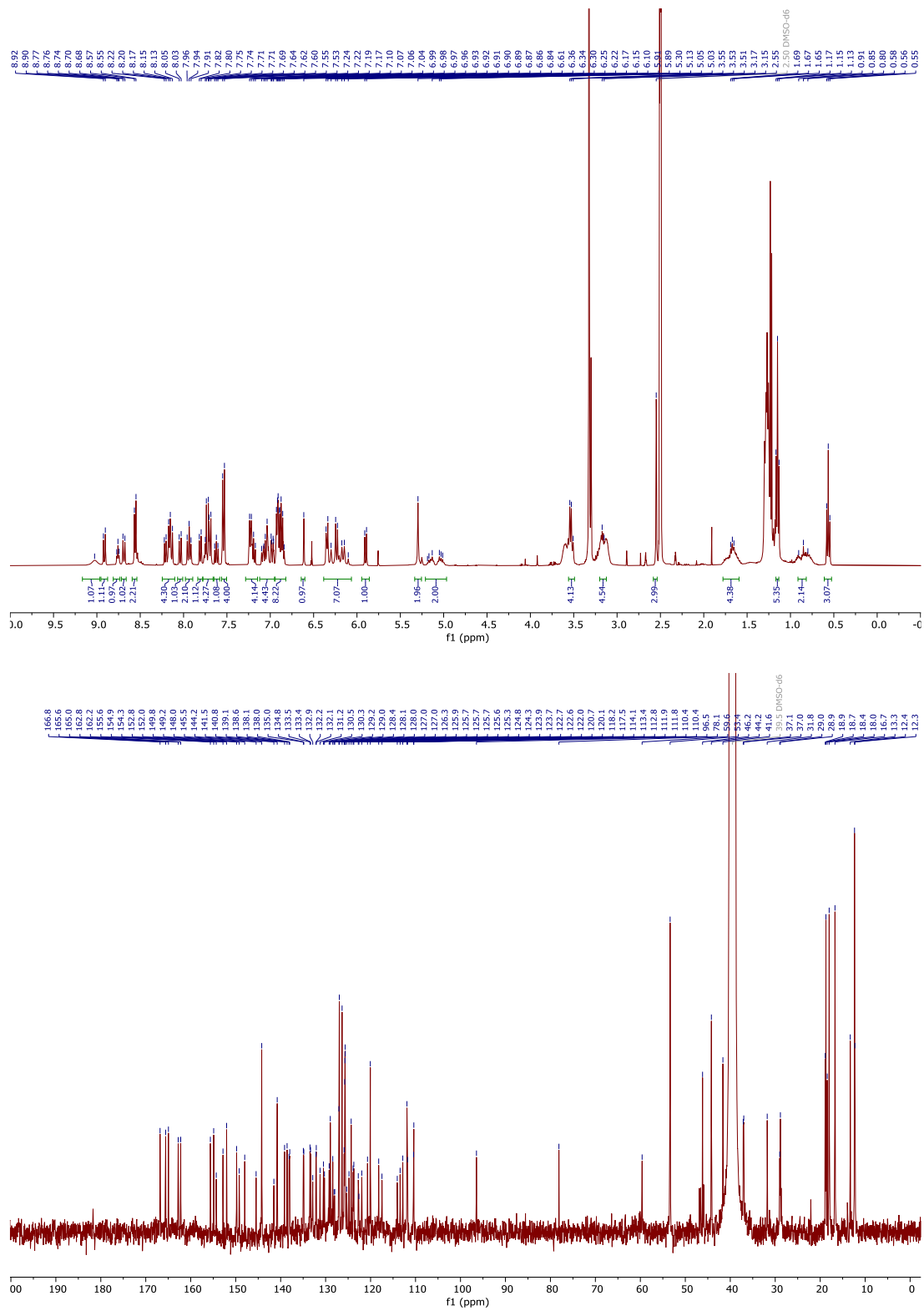


**Figure S3.** <sup>1</sup>H and <sup>13</sup>C NMR spectra of Ir(III)-COUPY conjugate **3c** in DMSO-*d*<sub>6</sub>.

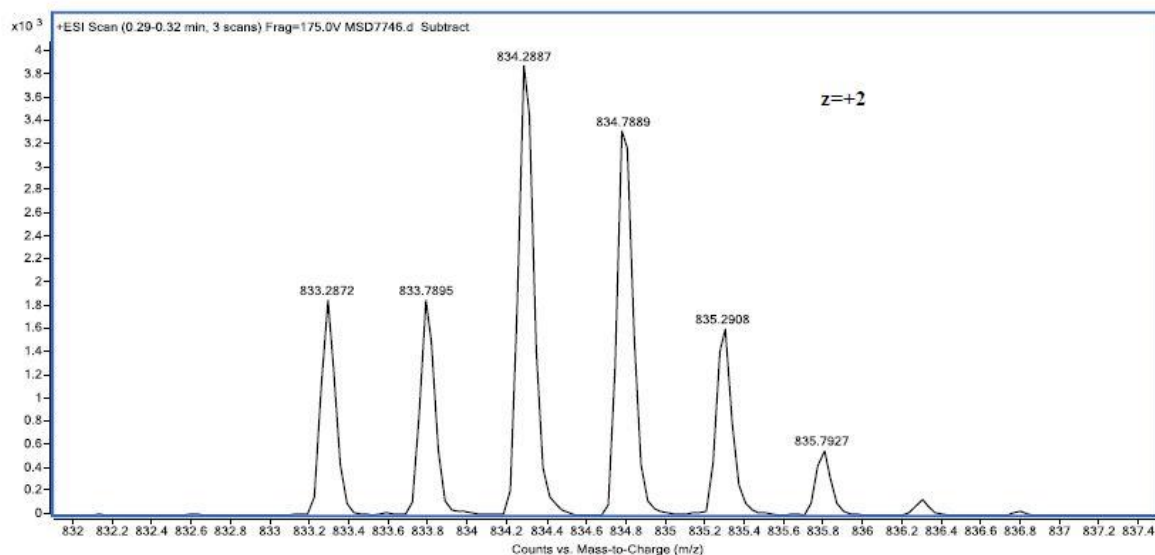
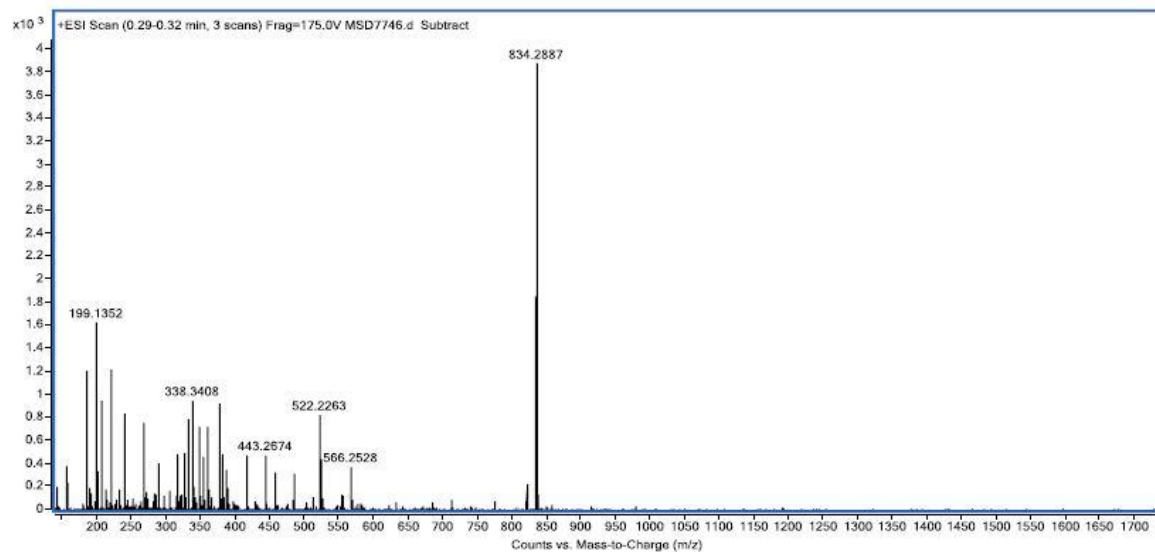


**Figure S4.** HR ESI-MS spectrum of Ir(III)-COUPY conjugate **3c**.

## 2.- Photophysical characterization of the compounds

**Table S1.** Photophysical and photochemical properties of the control compounds (coumarins **1a,1b** and Ir(III) complexes **2a,2b**) in different solvents at room temperature.

Comp.	Solvent	$\lambda_{\text{abs}}$ [nm]	$\epsilon$ [mM $\cdot$ cm $^{-1}$ ]	$\lambda_{\text{em}}$ [nm]	$\phi_f$ or $\phi_p$	$\tau_F$ [ns]	$\tau_P$ [ns]	$\Phi_\Delta$ at 355 nm	$\Phi_\Delta$ at 532 nm
<b>1a</b>	DCM	569	67	607	0.70	5.4	-	<0.01	0.03
	ACN	548	75	609	0.18	1.4	-	<0.01	<0.01
	PBS	545	34	604	0.14	0.9	-	$\approx$ 0	<0.01
<b>1b</b>	DCM	597	61	631	0.53	5.46	-	0.03	0.03
	ACN	572	60	635	0.22	2.03	-	$\approx$ 0	0.01
	PBS	557	38	629	0.031	0.031	-	$\approx$ 0	<0.01
<b>2a</b>	DCM	303	42	665	0.07	-	315	0.23	-
	ACN	302	41	660	0.03	-	187	0.42	-
	PBS	305	40	656	>0.01	-	55 (93%)	<0.01	-
<b>2b</b>	DCM	308	44	644	0.233	-	644	0.28	0.28
	ACN	305	44	650	0.127	-	331	0.42	0.43
	PBS	308	43	644	0.176	-	523	<0.01	<0.01

**Table S2.** Photophysical and photochemical properties of the Ir(III)-COUPY conjugates **3a-3c** in different solvents at room temperature.

Comp.	Solvent	$\lambda_{\text{abs}}$ [nm]	$\epsilon$ [mM $\cdot$ cm $^{-1}$ ]	$\lambda_{\text{em}}$ [nm]	$\phi_f$ or $\phi_p$	$\tau_F$ [ns]	$\tau_P$ [ns]	$\Phi_A$ at 355 nm	$\Phi_A$ at 532 nm
<b>3a</b>	DCM	566	44	602	0.07	0.25	121 (70%) 392 (30%)	0.37	0.34
	ACN	555	22	615	0.08	0.51	45 (86%) 269 (14%)	0.23	0.24
	PBS	550	17	615	0.004	0.37 (73%) 3.3 (27%)	-	<0.01	<0.01
<b>3b</b>	DCM	592	26	629	0.17	2.66	69 (80%) 298 (20%)	0.20	0.16
	ACN	580	24	647	0.08	0.9 (74%) 3.534 (26%)	264	0.14	0.12
	PBS	575	13	610	0.003	1.4	317 (78%) 43 (22%)	<0.01	<0.01
<b>3c</b>	DCM	565	50	599	0.24	4.17 (54%) 0.67 (46%)	198 (75%) 472 (25%)	0.34	0.27
	ACN	556	50	606	0.43	1.14 (76%) 15.05 (24%)	280 (73%) 039 (27%)	0.22	0.20
	PBS	544	22	611	0.027	0.82	306 (60%) 292 (40%)	<0.01	<0.01

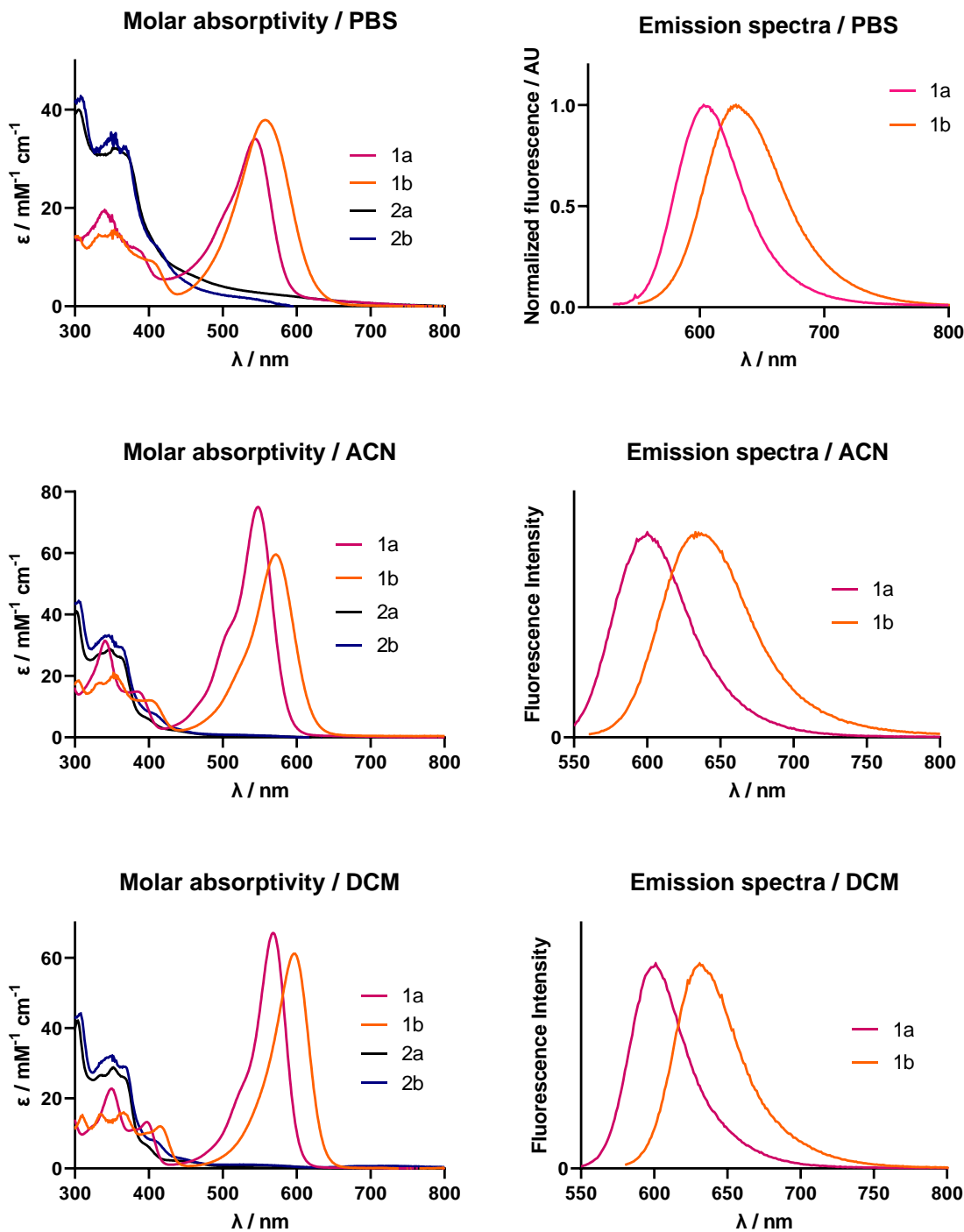


**Figure S5.** Comparison of the absorption (left) and emission spectra (right) of COUPY dyes **1a,1b**, and Ir(III) complexes **2a,2b** in PBS (top), ACN (center) and DCM (bottom).

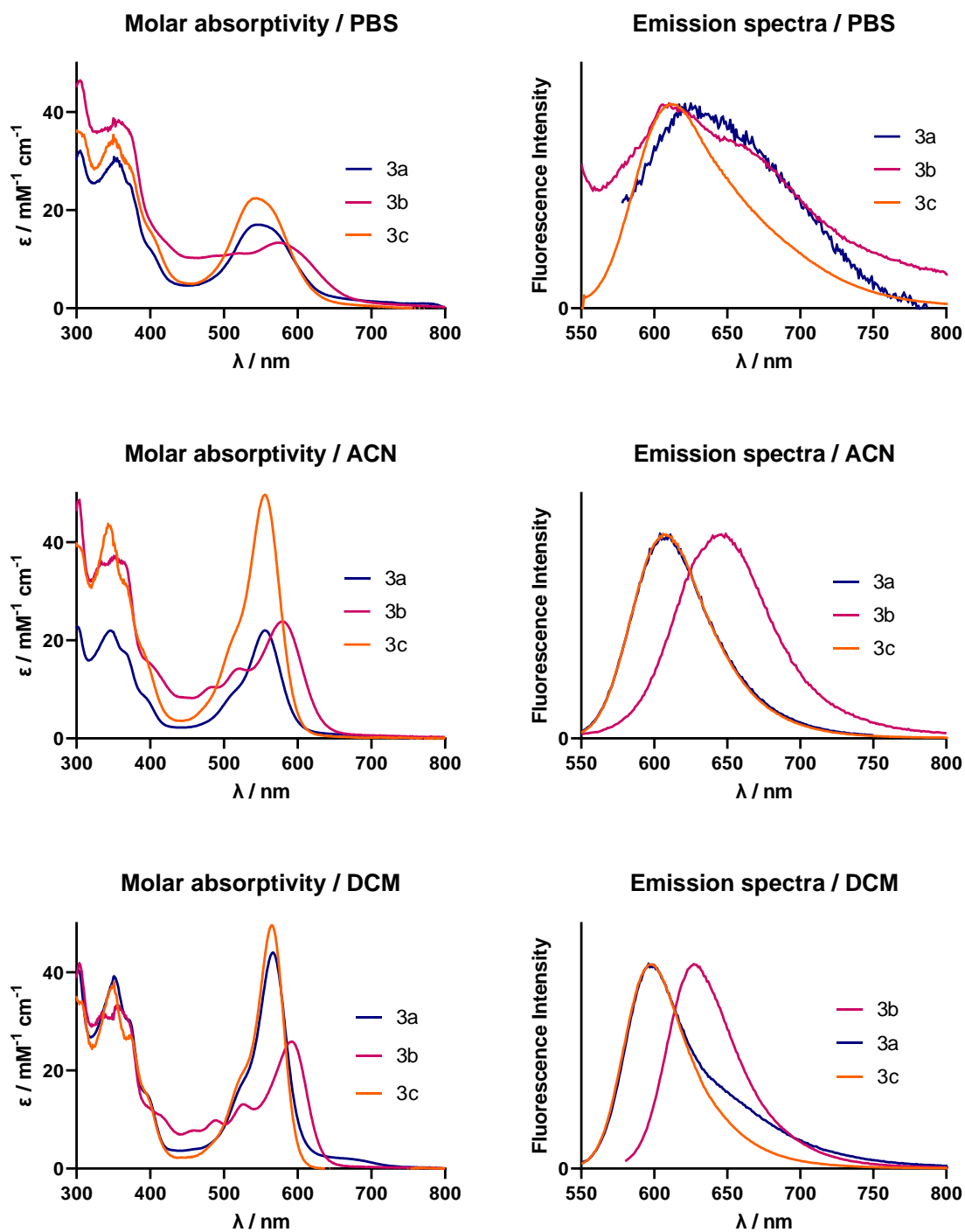


**Figure S6.** Comparison of the absorption (left) and emission spectra (right) of conjugates **3a**-**3c** in PBS (top), ACN (center) and DCM (bottom).

### 3.- Photochemical characterization of the compounds

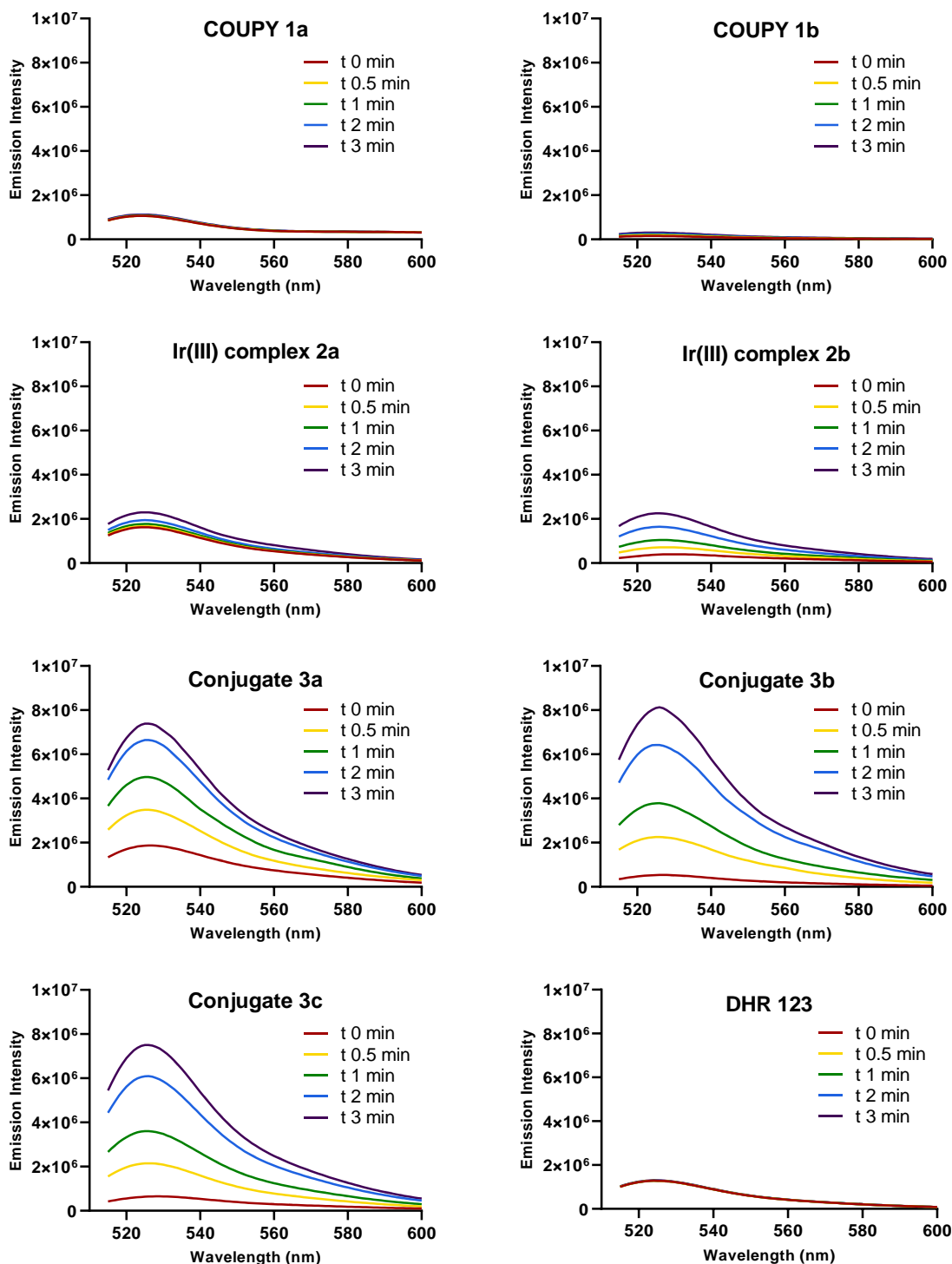


**Figure S7.** Fluorescence spectra of DHR123 induced by irradiation with red light ( $620\pm15$  nm;  $130$  mW cm $^{-2}$ ) in the presence of COUPY dyes **1a**, **1b**, Ir(III) complexes **2a**, **2b**, Ir(III)-COUPY conjugates **3a**-**3c** or without any compound (DHR 123 alone).

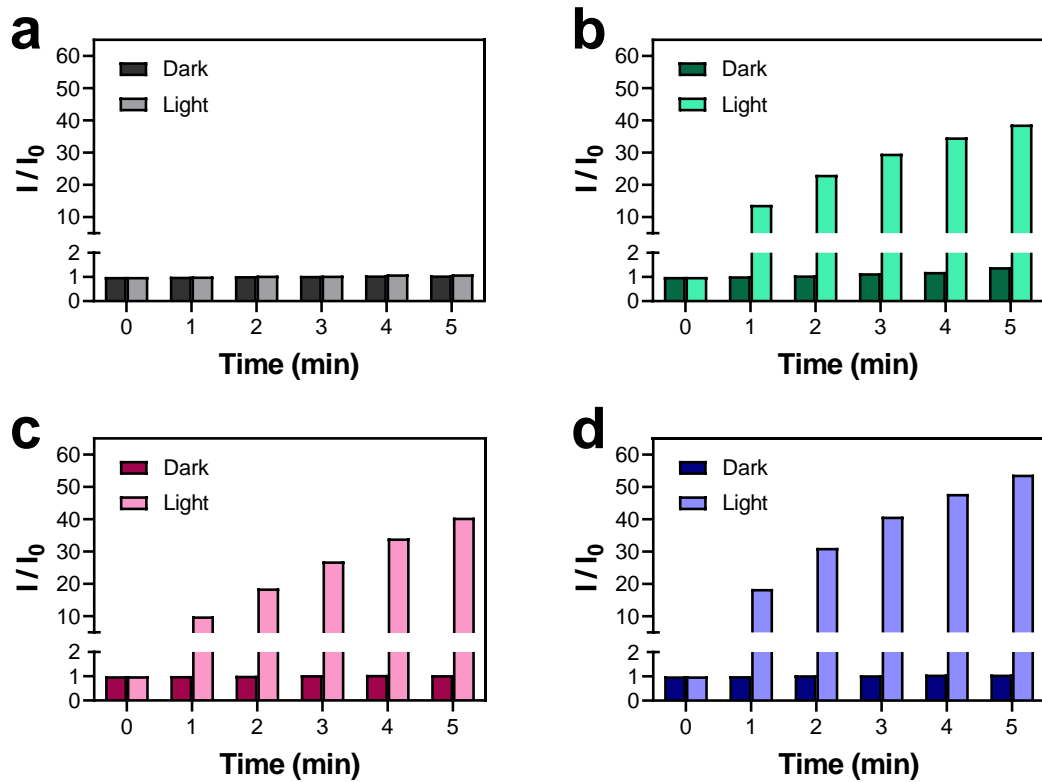


**Figure S8.** Photogeneration of superoxide anion radical ( $O_2^{\bullet-}$ ) by Ir(III)-COUPY conjugates **3a-3c** in PBS. DHR123 (10  $\mu$ M) was used to detect the generation of  $O_2^{\bullet-}$  in the absence (a) and in the presence of compounds **3a** (b), **3b** (c) and **3c** (d) (10  $\mu$ M) in PBS (2 % DMSO), before and upon irradiation with red light ( $620\pm15$  nm; 130 mW  $cm^{-2}$ ).

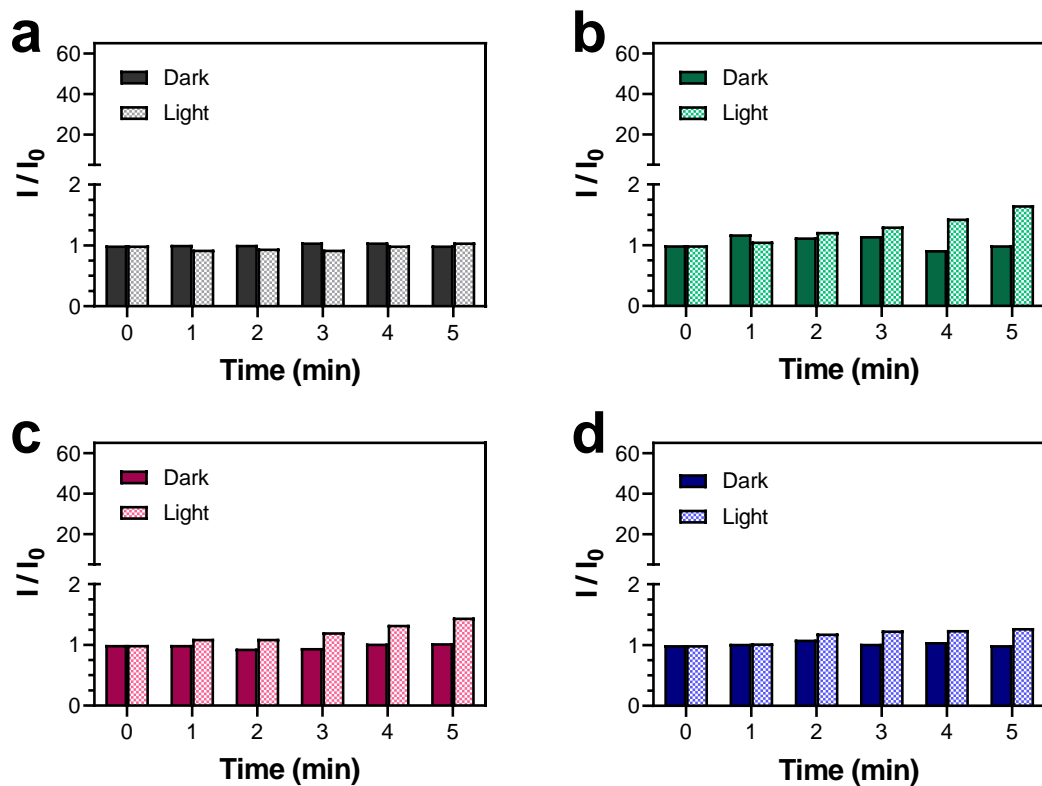


**Figure S9.** Quenching the photogeneration of  $\text{O}_2^{\cdot-}$  by Ir(III)-COUPY conjugates **3a-3c** using tiron as a scavenger. DHR123 (10  $\mu\text{M}$ ) was used to detect the generation of  $\text{O}_2^{\cdot-}$  in the absence (a) and in the presence of compounds **3a** (b), **3b** (c) and **3c** (d) (10  $\mu\text{M}$ ) in tiron-saturated PBS (2 % DMSO), before and upon irradiation with red light ( $620\pm15\text{ nm}$ ;  $130\text{ mW cm}^{-2}$ ).

**Table S3.** Adiabatic electron affinity and ionization potential (EA and IP), in eV. The O<sub>2</sub> electron affinity (-3.42 eV) at the same level of theory was taken from *Chem Sci*, 2020, 11, 9784–9806.

Molecule	EA	IP	$\Delta E(S_0 \rightarrow S_1)^a$
<sup>1</sup> 1a <sup>+</sup>		5.433	2.275
<sup>1</sup> 1b <sup>+</sup>		5.185	2.226
<sup>1</sup> 2a <sup>+</sup>	-3.257		
<sup>1</sup> 2b <sup>+</sup>	-3.261		

<sup>a</sup> Experimental absorption band maximum in PBS.

**Table S4.** Energy difference between products and reactants ( $\Delta E$ ) for the electron transfer (COUPY→Ir(III) complex) in absence of light. Units in eV.

#	Reaction	Thermodynamic calculation	System	$\Delta E$
(1)	<sup>1</sup> 1a <sup>+</sup> (S0) + <sup>1</sup> 2a <sup>+</sup> → <sup>2</sup> 1a <sup>2+</sup> + <sup>2</sup> 2a <sup>0</sup>	IP ( <sup>1</sup> 1a <sup>+</sup> ) + EA ( <sup>1</sup> 2a <sup>+</sup> )	3a	2.176
(2)	<sup>1</sup> 1b <sup>+</sup> (S0) + <sup>1</sup> 2a <sup>+</sup> → <sup>2</sup> 1b <sup>2+</sup> + <sup>2</sup> 2a <sup>0</sup>	IP ( <sup>1</sup> 1b <sup>+</sup> ) + EA ( <sup>1</sup> 2a <sup>+</sup> )	3b	1.928
(3)	<sup>1</sup> 1a <sup>+</sup> (S0) + <sup>1</sup> 2b <sup>+</sup> → <sup>2</sup> 1a <sup>2+</sup> + <sup>2</sup> 2b <sup>0</sup>	IP ( <sup>1</sup> 1a <sup>+</sup> ) + EA ( <sup>1</sup> 2b <sup>+</sup> )	3c	2.172

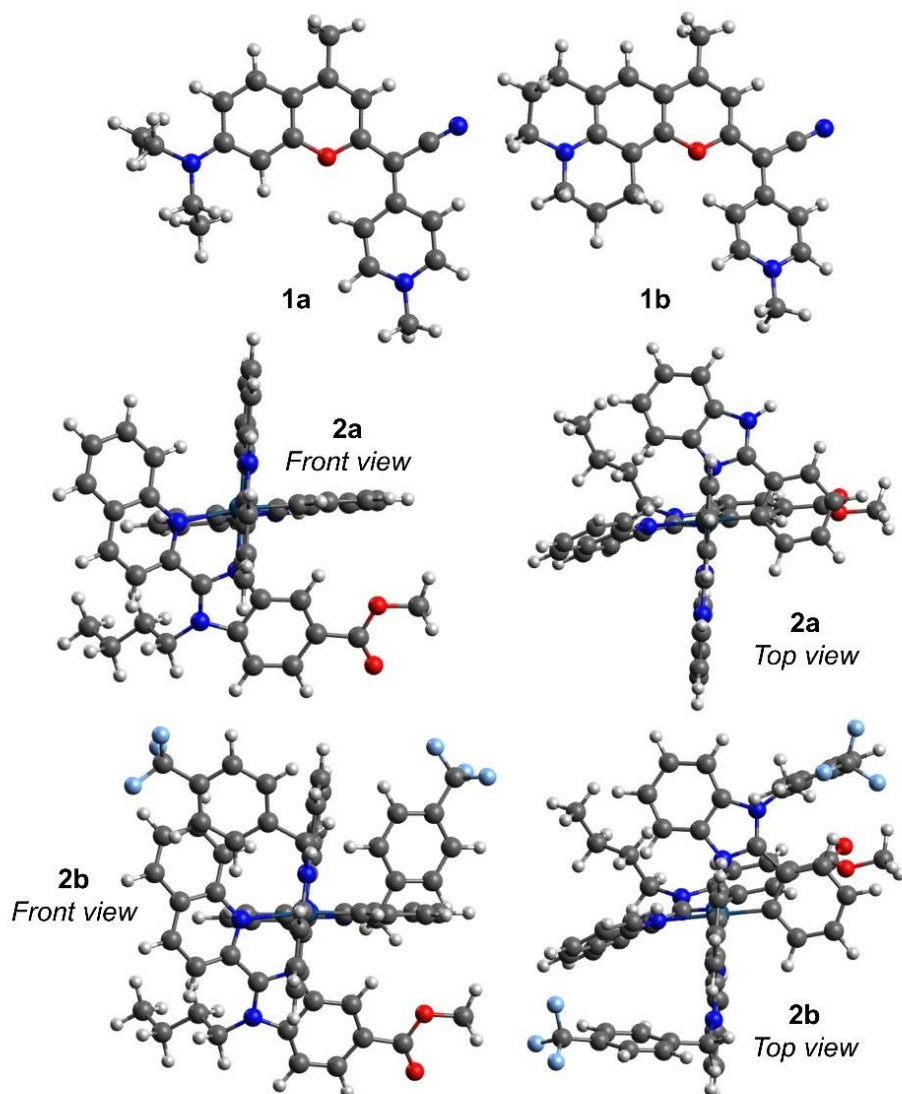


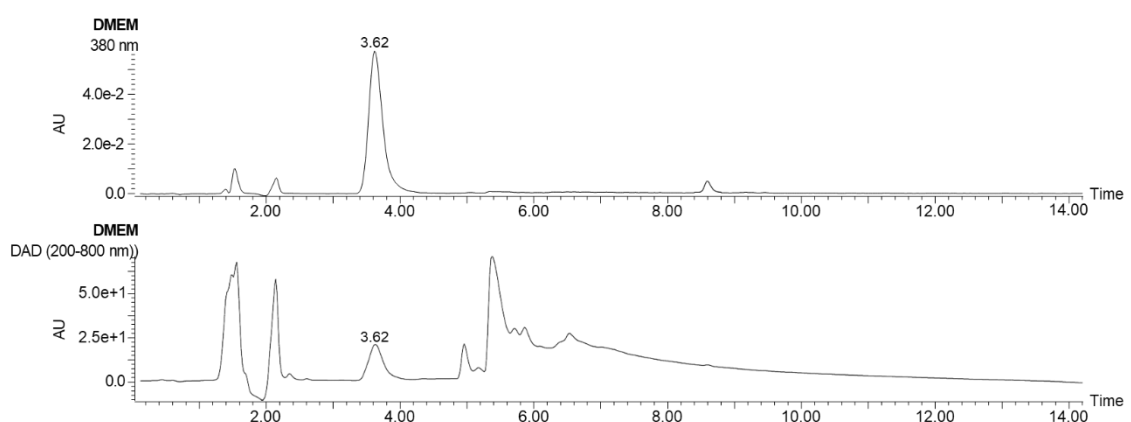
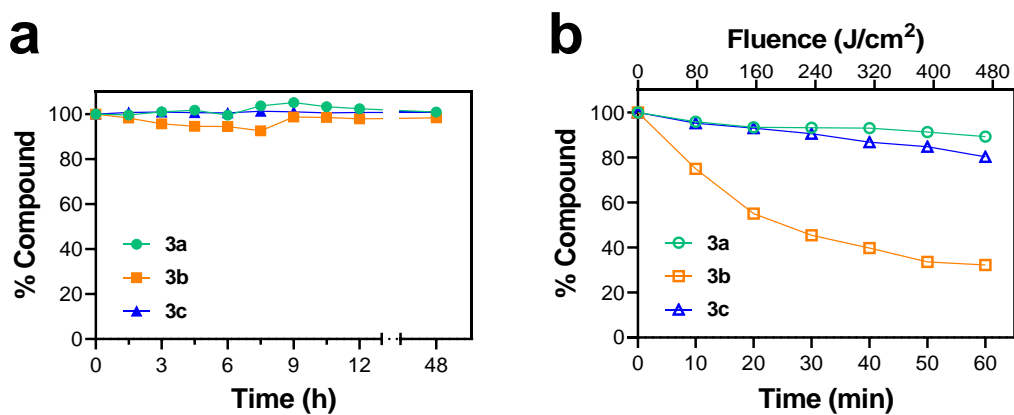
**Figure S10.** 3D models of the ground-state structures of **1a**, **1b**, **2a**, and **2b**.

#### **4.- Dark and light stability of Ir(III)-COUPY conjugates in biological medium**

For the dark stability studies, 1.5 mL of a solution of the corresponding Ir(III)-COUPY conjugate (20  $\mu$ M) in DMEM culture medium supplemented with 10% FBS, 2 mM L-glutamine and 100 U·mL<sup>-1</sup> of penicillin-streptomycin mixture was stirred in a thermomixer (800 rpm, 37 °C) for 48 h. A 60  $\mu$ L aliquot of the previous solution was taken after the indicated time intervals (0, 1.5, 3, 4.5, 6, 7.5, 9, 10.5, 12 and 48 h) and analysed by reversed-phase HPLC. The extent of degradation of the PS was determined by calculating the ratio between the peak area of the compound and that of DMEM peak at 3.62 min, before and after incubation for the indicated time interval.

For the photostability studies, 1.5 mL of a solution of the corresponding Ir(III)-COUPY conjugate (20  $\mu$ M) in DMEM culture medium supplemented with 10% FBS, 2 mM L-glutamine and 100 U·mL<sup>-1</sup> of penicillin-streptomycin mixture was irradiated with red light (620±15 nm; 130 mW cm<sup>-2</sup>) for up to 1 h at 37 °C. A 60  $\mu$ L aliquot of the previous solution was taken after irradiation for the indicated time intervals (0, 10, 20, 30, 40, 50 and 60 min) and analysed by reversed-phase HPLC. The extent of photodegradation of the PS was determined by calculating the ratio between the peak area of the Ir(III) complex and that of DMEM peak at 3.62 min, before and after irradiation for the indicated time interval.

The HPLC analysis was performed with a Waters alliance 2695 Separations Module, comprised of a quaternary pump solvent delivery module, online degasser, auto sampler and a Waters 2996 photodiode array detector. HPLC separation was carried out using a Jupiter Proteo C12 column (150 x 4.6 mm, 90 Å, 4  $\mu$ m) from Phenomenex. The mobile phase was a linear gradient beginning with 70:30 (v/v) A/B and ending with 0:100 (v/v) A/B over 15 min at a flow rate of 1 mL/min (A: 0.05% TFA in H<sub>2</sub>O; B: 0.05% TFA in ACN). The injection volume was 40  $\mu$ L. Control of the HPLC instrument, as well as processing of the chromatogram output (annotation of retention times, integration of peaks, calculation of peak areas) was carried out with MassLynx V4.1 software. Elution traces were obtained at 380 nm.



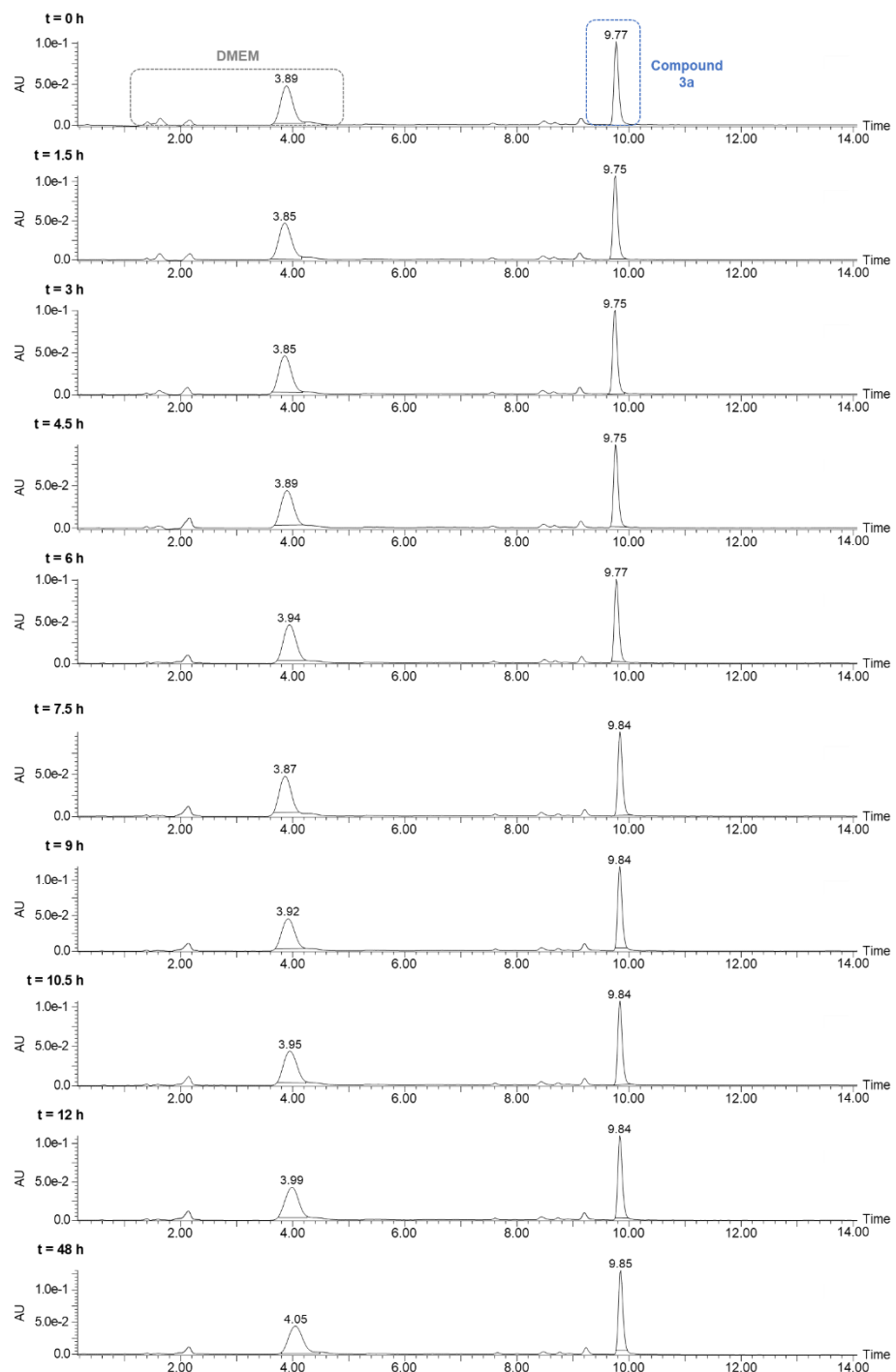


**Figure S13:** Stability of compound **3a** in cell culture medium. From top to bottom: HPLC chromatograms of **3a** (20  $\mu$ M) in DMEM before incubation ( $t = 0$  h) and after incubation at 37 °C during 1.5, 3, 4.5, 6, 7.5, 9, 10.5, 12 and 48 h, respectively. Elution traces obtained at 380 nm.

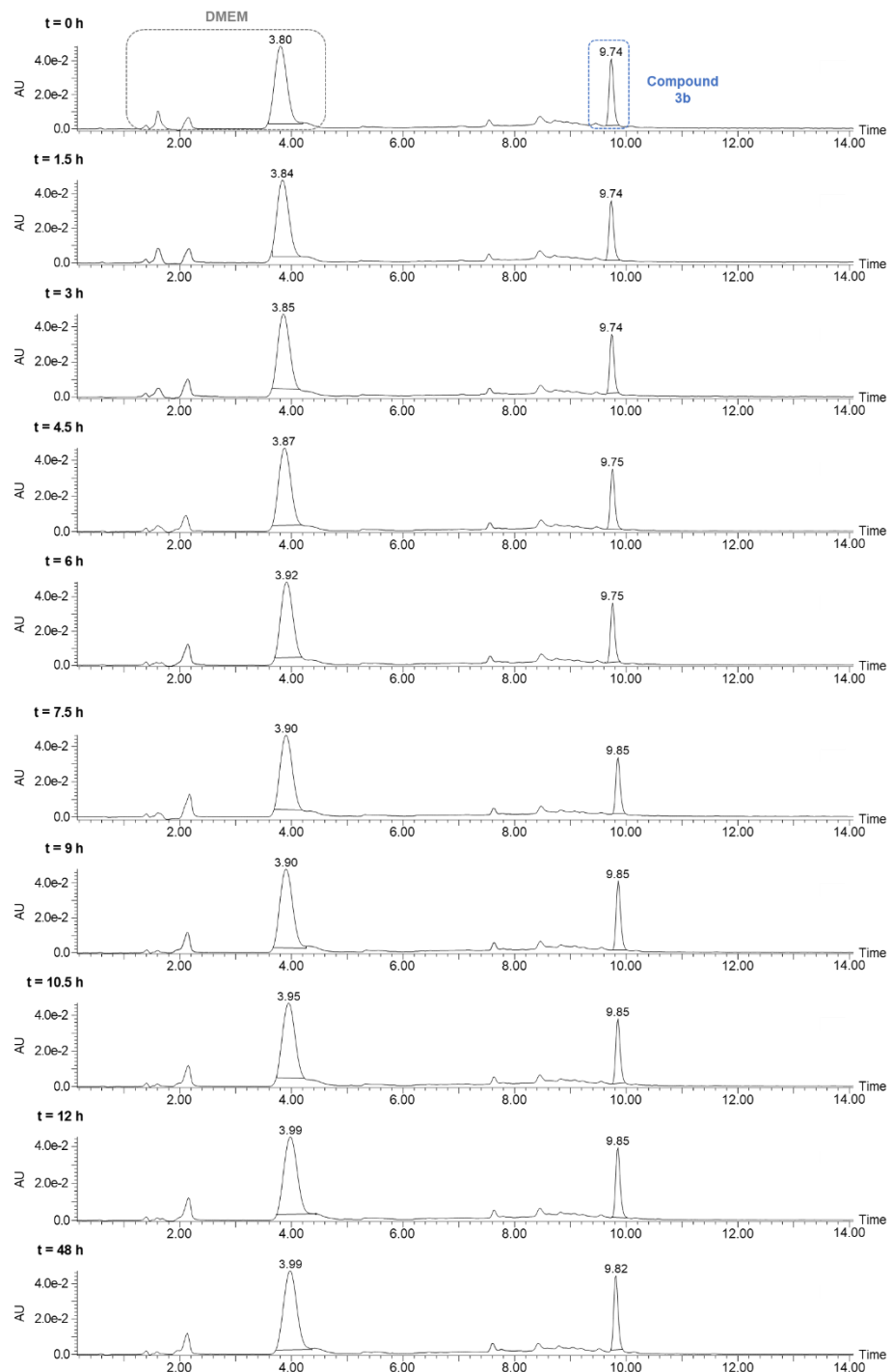


**Figure S14:** Stability of compound **3b** in cell culture medium. From top to bottom: HPLC chromatograms of **3b** (20  $\mu$ M) in DMEM before incubation ( $t = 0$  h) and after incubation at 37 °C during 1.5, 3, 4.5, 6, 7.5, 9, 10.5, 12 and 48 h, respectively. Elution traces obtained at 380 nm.

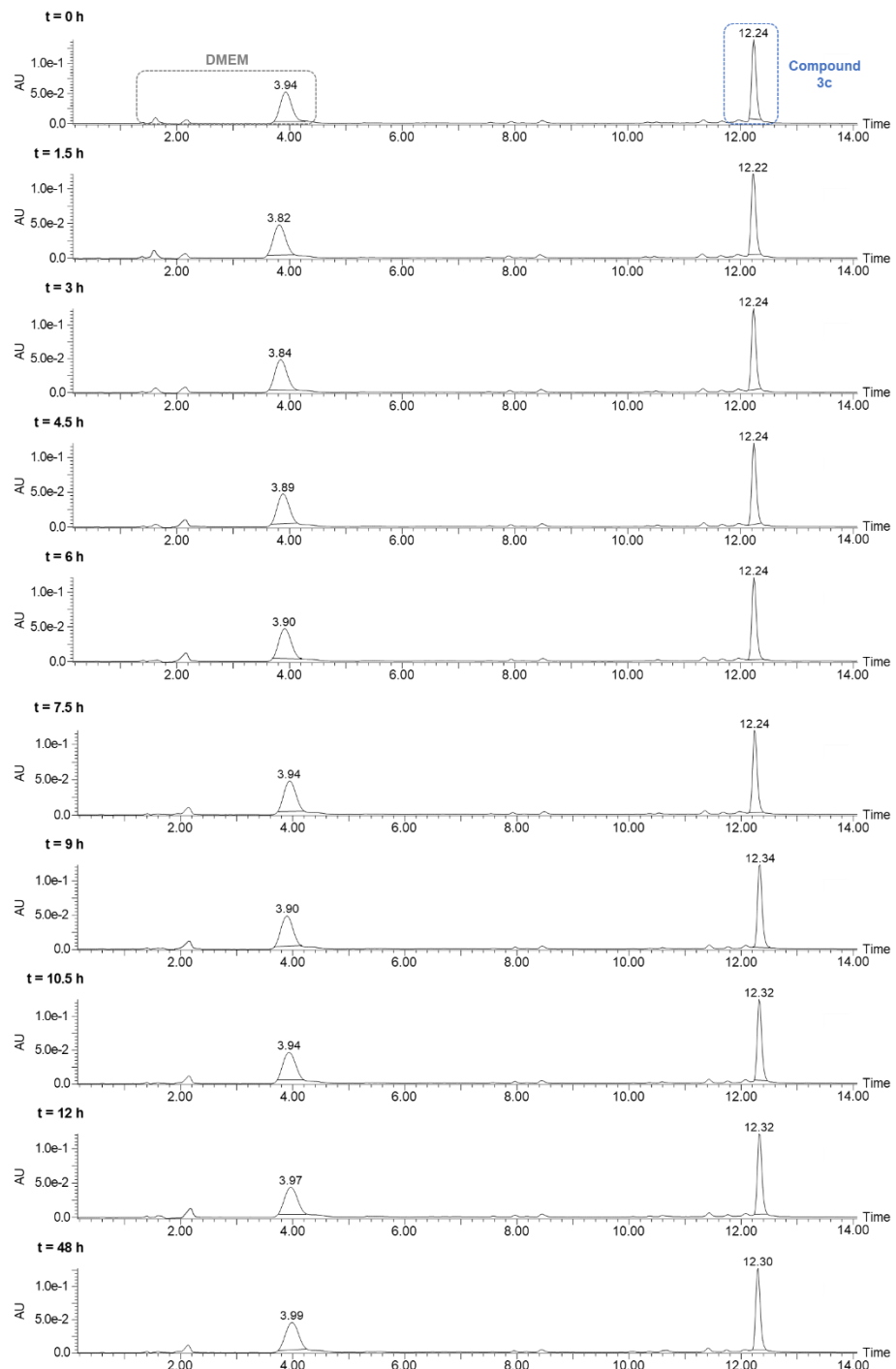


**Figure S15:** Stability of compound **3c** in cell culture medium. From top to bottom: HPLC chromatograms of **3c** (20  $\mu$ M) in DMEM before incubation ( $t = 0$  h) and after incubation at 37 °C during 1.5, 3, 4.5, 6, 7.5, 9, 10.5, 12 and 48 h, respectively. Elution traces obtained at 380 nm.

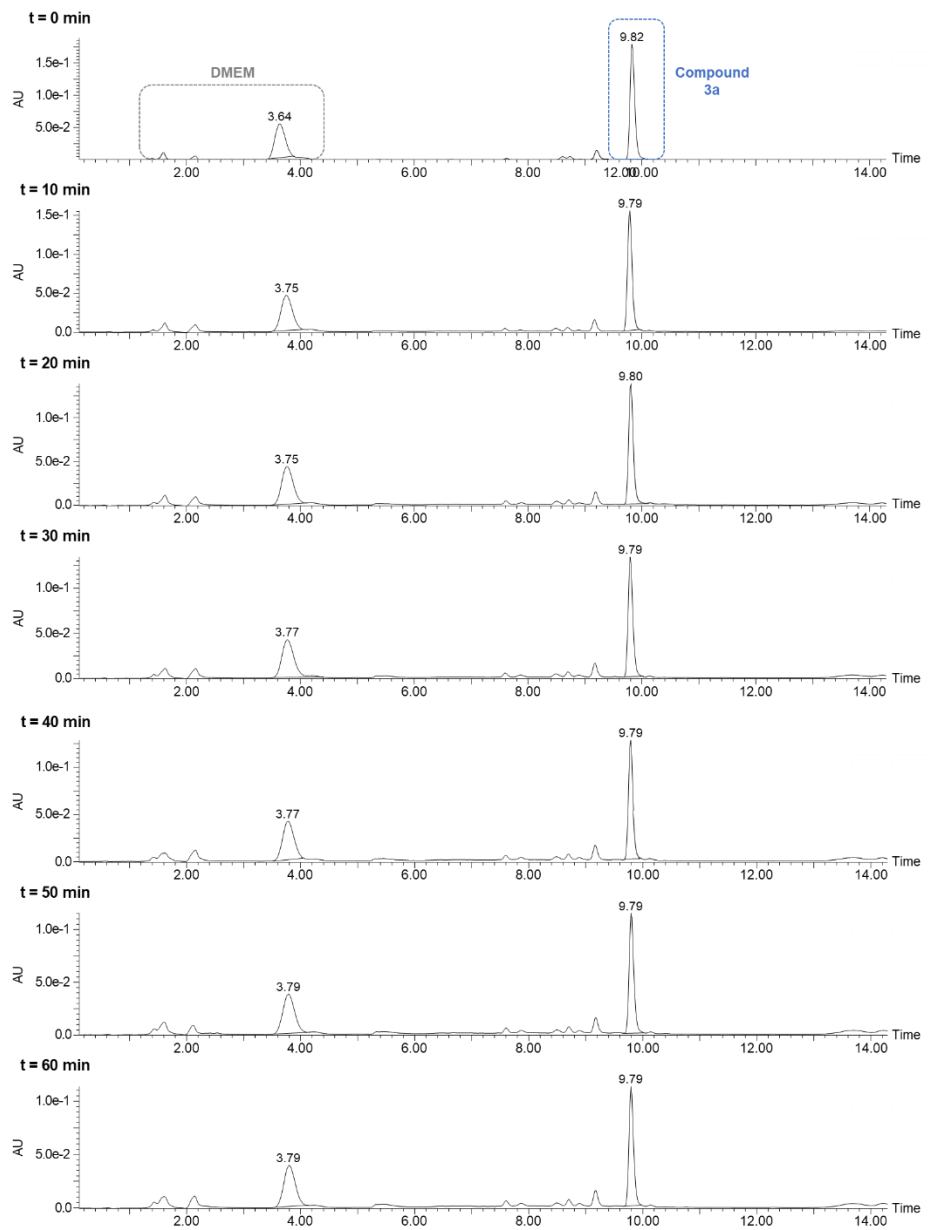


**Figure S16:** Photostability of compound **3a** in cell culture medium upon irradiation with red light. From top to bottom: HPLC chromatograms of **3a** (20  $\mu$ M) in DMEM before irradiation ( $t = 0$  min) and after irradiation with red light ( $620 \pm 15$  nm;  $130$  mW cm $^{-2}$ ) for up to 1 h (10, 20, 30, 40, 50 and 60 min, respectively) at 37 °C. Elution traces were obtained at 380 nm.

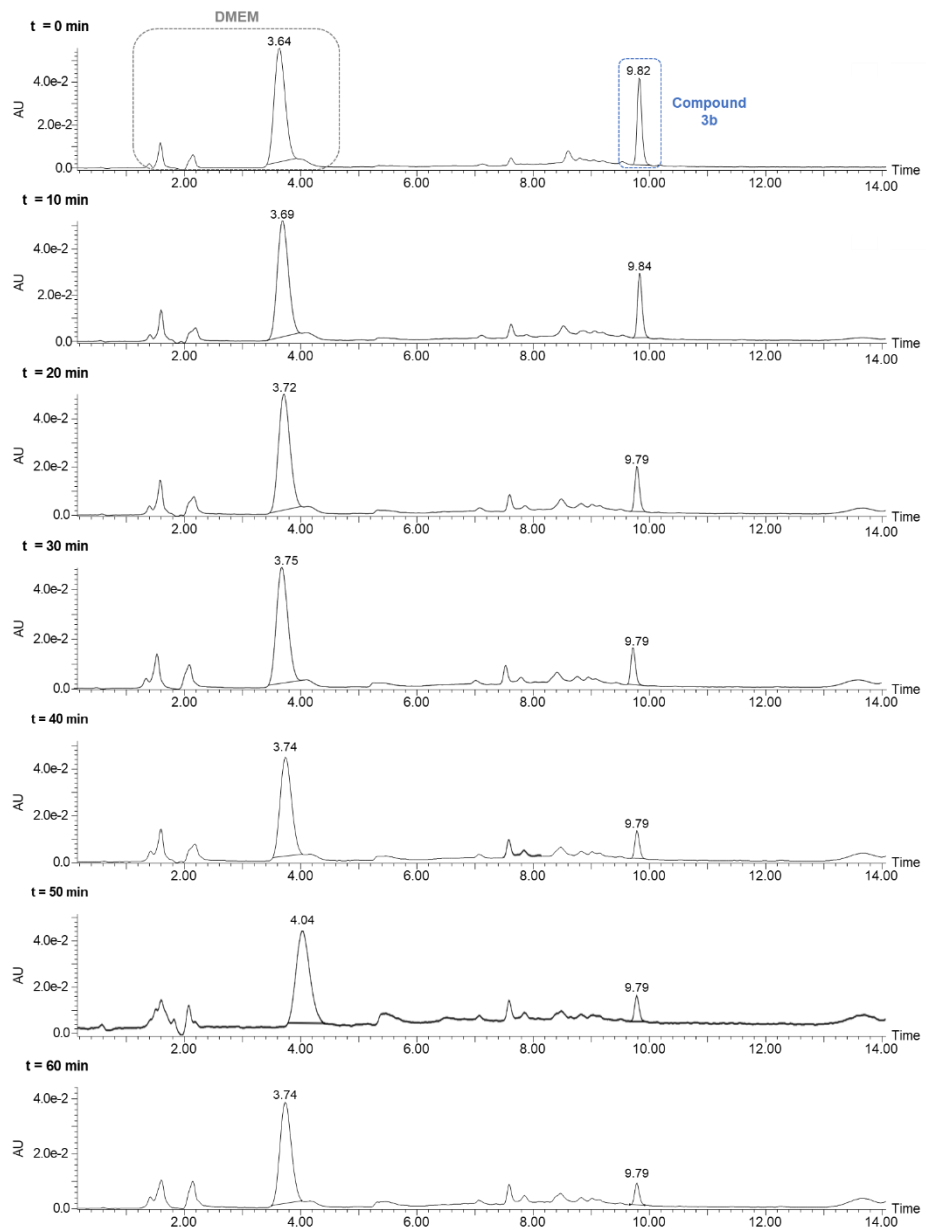


**Figure S17:** Photostability of compound **3b** in cell culture medium upon irradiation with red light. From top to bottom: HPLC chromatograms of **3b** (20  $\mu$ M) in DMEM before irradiation ( $t = 0$  min) and after irradiation with red light ( $620\pm15$  nm;  $130$  mW cm $^{-2}$ ) for up to 1 h (10, 20, 30, 40, 50 and 60 min, respectively) at 37 °C. Elution traces were obtained at 380 nm.

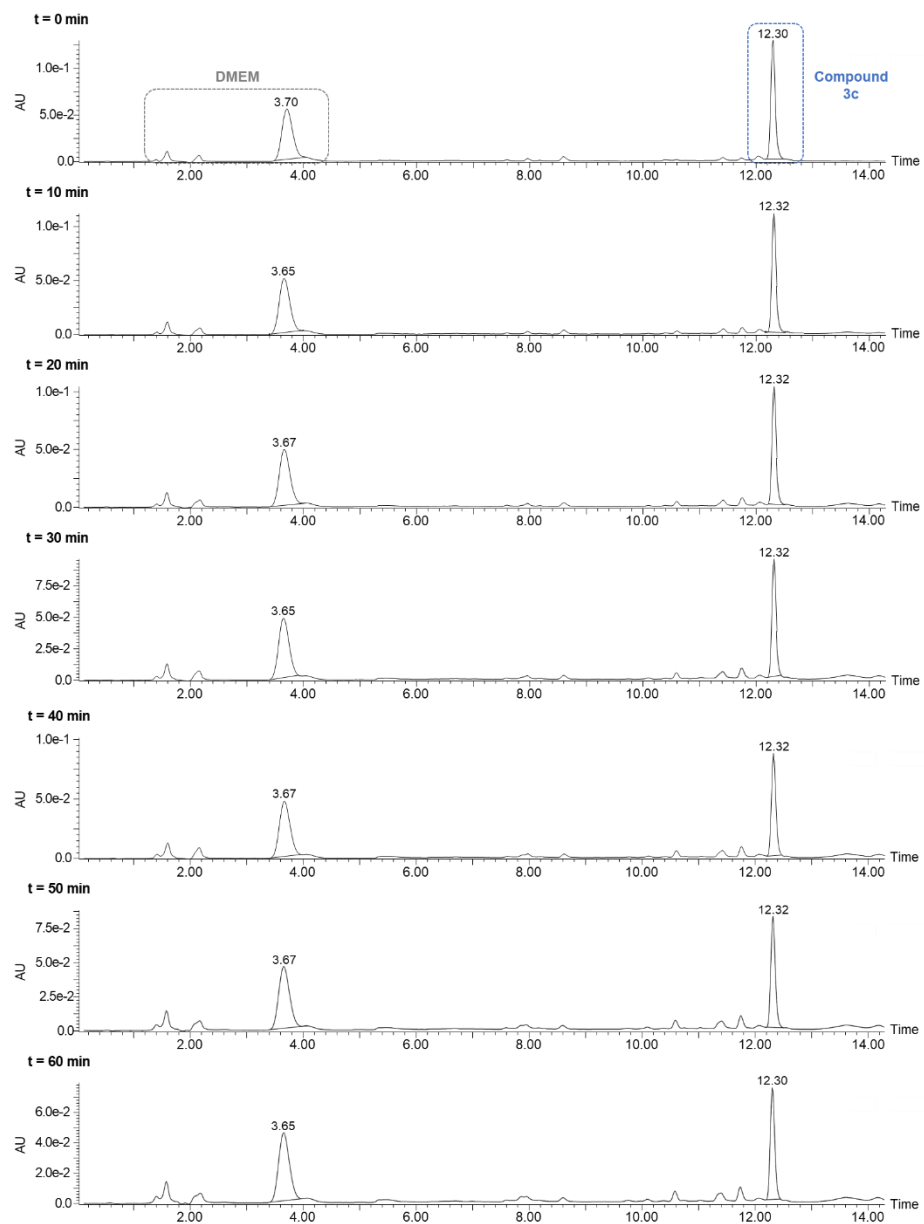


**Figure S18:** Photostability of compound **3c** in cell culture medium upon irradiation with red light. From top to bottom: HPLC chromatograms of **3c** (20  $\mu$ M) in DMEM before irradiation ( $t = 0$  min) and after irradiation with red light ( $620\pm15$  nm;  $130$  mW  $\text{cm}^{-2}$ ) for up to 1 h (10, 20, 30, 40, 50 and 60 min, respectively) at  $37^\circ\text{C}$ . Elution traces were obtained at 380 nm.

## 5.- Fluorescence imaging by confocal microscopy and accumulation studies by ICP-MS

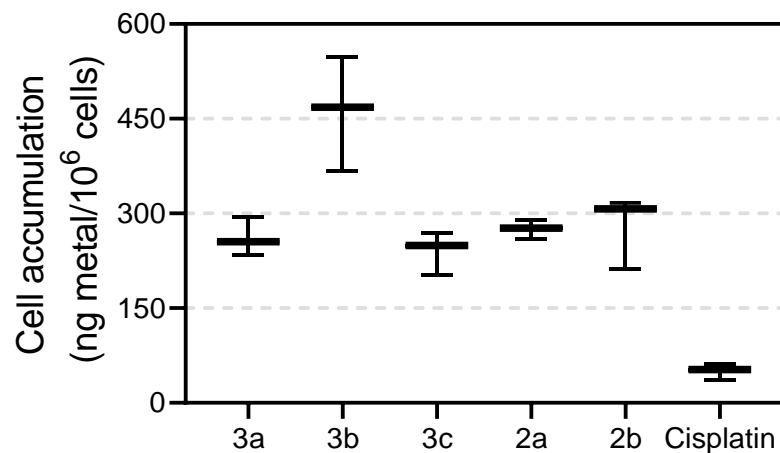


**Figure S19.** Total cellular accumulation (ng Ir or Pt/10<sup>6</sup> cells) of Ir compounds or cisplatin in A2780cis cells after 2 h treatment at 10  $\mu$ M. Data expressed as mean  $\pm$  SD from three independent measurements.

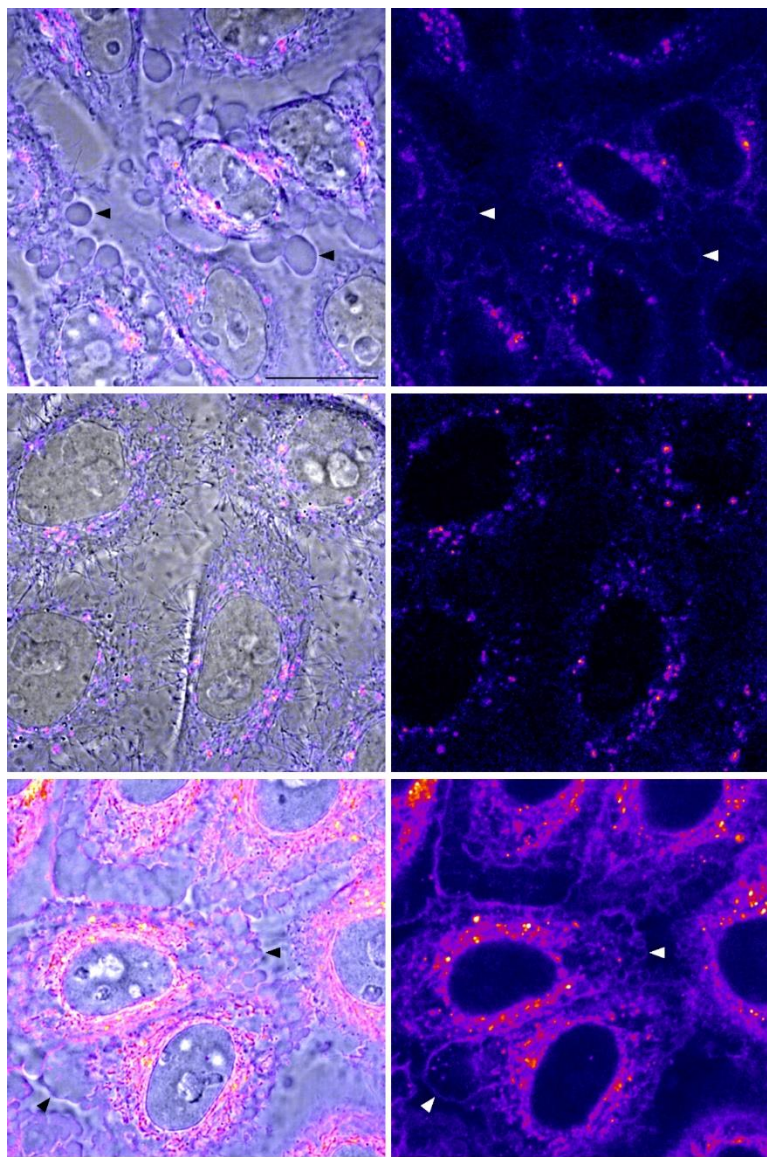


**Figure S20.** Confocal sections of HeLa cells incubated with **3a** (top), **3b** (middle) and **3c** (bottom) merged with the brightfield images (left) or showing fluorescence signal alone (right). Black and white arrowheads point out cell blebbings. Scale bar: 20  $\mu\text{m}$ . Same scale on all images.

**Table S5:** Pearson's correlation coefficient (PCC) values between Ir(III)-COUPY conjugates **3a**-**3c** and Wheat Germ Agglutinin Alexa Fluor 633 (WGA), or Lysotracker Green DND (LTG). For WGA, the value outside the parentheses represents the result from the correlation between the global signal of the WGA channel (extracellular membrane and endosomes) and that of the compound, while the value inside the parentheses represents the result from the specific analysis of the vesicular component of these two channels. n ≥ 26 cells for each compound.

Compound	WGA	LTG
<b>3a</b>	0.695 (0.421)	0.065
<b>3b</b>	0.514 (0.437)	0.034
<b>3c</b>	0.685 (0.359)	0.117

## 6.- Photobiological evaluation

**Table S6 .** Photocytotoxicity towards A2780cis cells under normoxia and hypoxia.<sup>a</sup>

	Normoxia			Hypoxia		
	<b>IC<sub>50</sub> (µM)</b> <b>Dark</b>	<b>IC<sub>50</sub> (µM)</b> <b>620 nm</b>	<b>PI<sup>b</sup></b>	<b>IC<sub>50</sub> (µM)</b> <b>Dark</b>	<b>IC<sub>50</sub> (µM)</b> <b>620 nm</b>	<b>PI<sup>b</sup></b>
<b>1a</b>	>250	7.1 ± 0.4	>35	>250	5.9 ± 0.9	>42.4
<b>1b</b>	15 ± 2	0.7 ± 0.1	21.4	34 ± 5	0.37 ± 0.04	91.9
<b>2a</b>	>250	4.5 ± 0.3	>56	>250	n.d.	n.d.
<b>2b</b>	>250	9 ± 2	>28	>250	n.d.	n.d.
<b>3a</b>	>250	0.71 ± 0.02	>352	>250	1.6 ± 0.2	>156
<b>3b</b>	>250	1.2 ± 0.1	>208	>250	5 ± 1	>50
<b>3c</b>	>250	1.2 ± 0.2	>208	>250	1.4 ± 0.5	>179
<b>5-ALA</b>	>250	34 ± 8	>7	>250	>250	-

<sup>a</sup>Cells were treated for 2 h (1 h incubation and 1 h irradiation with red light) followed by 48 h of incubation in drug-free medium either under normoxic (21% O<sub>2</sub>) or hypoxic (2% O<sub>2</sub>) conditions. Dark analogues were kept in the dark. Data expressed as mean ± SD from three independent experiments.

<sup>b</sup>PI = phototherapeutic index defined as IC<sub>50</sub> (dark-non-irradiated cells)/IC<sub>50</sub> (irradiated cells).

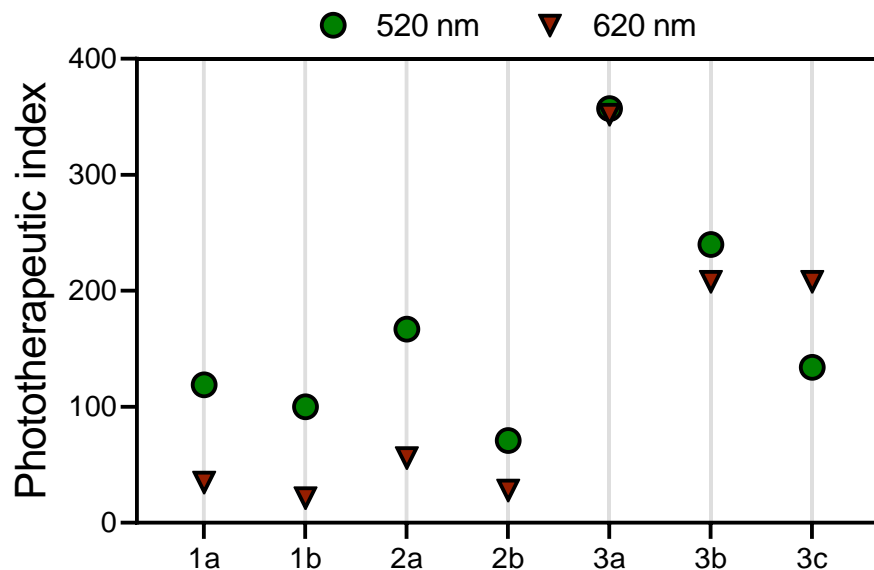


**Figure S21.** Summary of phototherapeutic indices (PI; IC<sub>50</sub> (dark)/IC<sub>50</sub>(light) in A2780cis under normoxia following green light (520 nm, 1.5 mW cm<sup>-2</sup>, 1 h) or red light (620 nm, 15 mW cm<sup>-2</sup>, 1 h) irradiation.

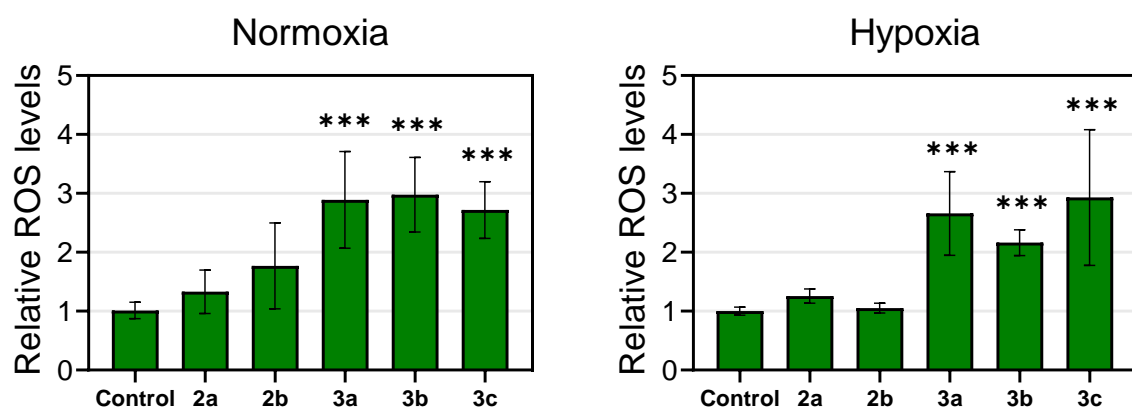


**Figure S22.** Relative ROS levels in A2780cis cells under normoxia (21% O<sub>2</sub>) and hypoxia (2% O<sub>2</sub>) after treatment with the investigated compounds at 10 µM in dark or upon light irradiation (620 nm, 90mW cm<sup>-2</sup>, 1 h) as measured with the DCFH-DA probe by flow cytometry. Data expressed as mean ± SD from three independent measurements.

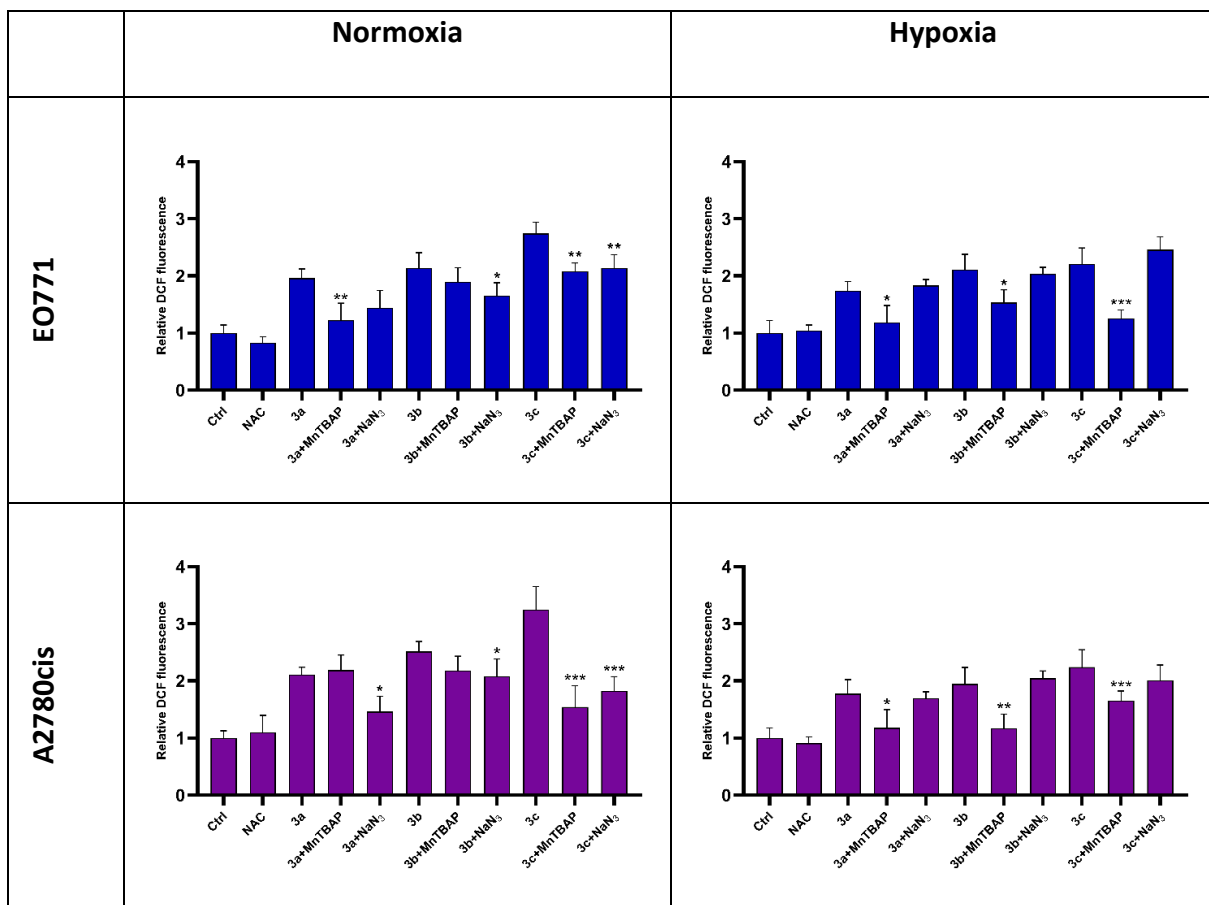


**Figure S23.** Relative ROS levels in EO771 and A2780cis cells under normoxia (21% O<sub>2</sub>) and hypoxia (2% O<sub>2</sub>) after treatment with the Ir(III)-COUPY **3a-3c** at 10 μM and/or co-treated with MnTBAP and NaN<sub>3</sub> upon light irradiation (620 nm, 15 mW cm<sup>-2</sup>, 1 h) as measured with the DCFH-DA probe. Statistical significance was determined relative to the treatment with conjugates alone and indicated by \*p < 0.05, \*\*p < 0.01, and \*\*\*p < 0.001 using two-way ANOVA. Data represented as mean ± SD (n = 2 replicates).

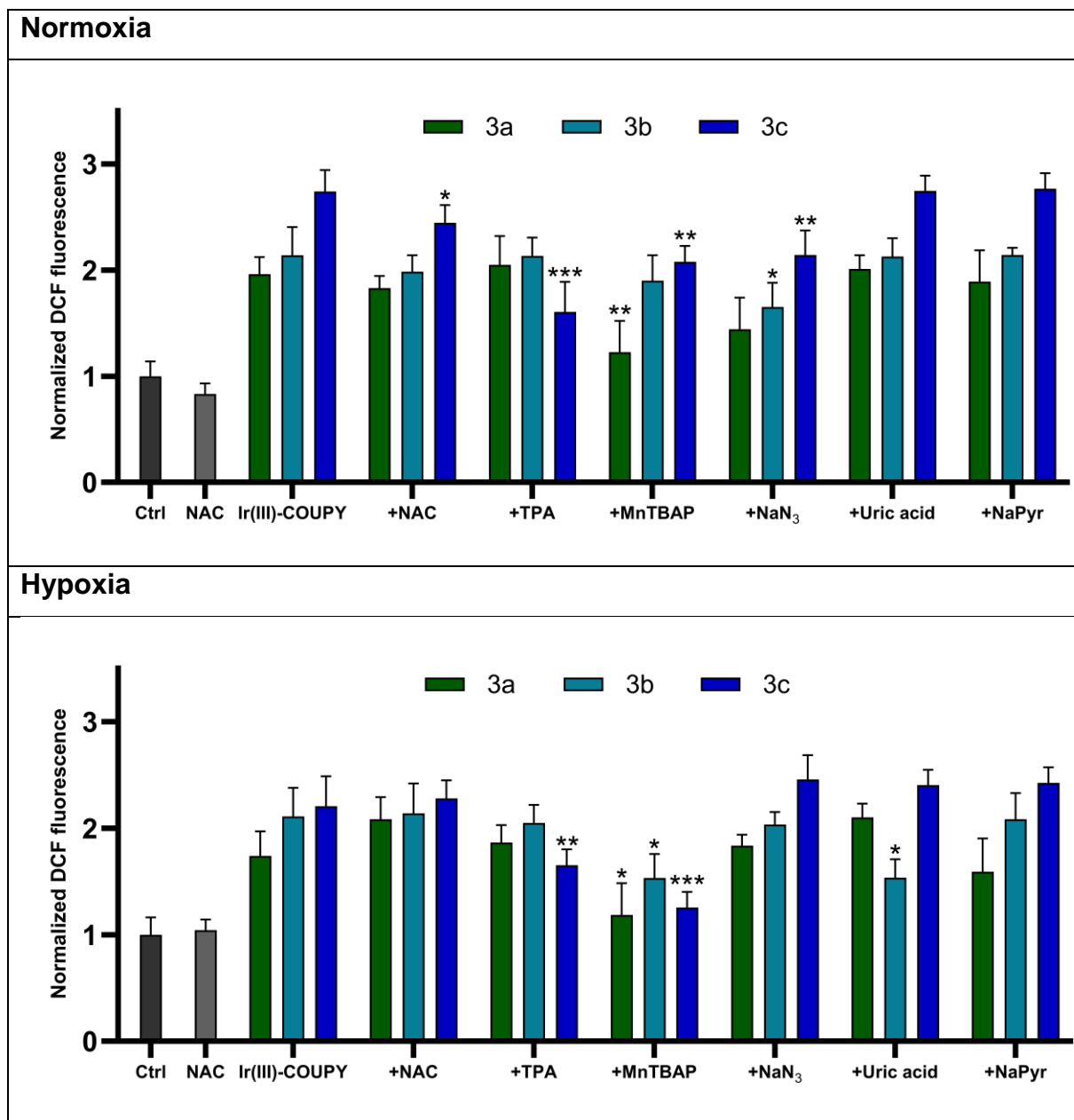


**Figure S24.** ROS levels in E0771 cells upon irradiation in normoxia (21% O<sub>2</sub>) and hypoxia (2% O<sub>2</sub>) treatments with 10 μM of the Ir(III)-COUPY conjugates **3a**, **3b** and **3c** and/or co-treated with the mentioned scavengers (1 h in the dark, followed by 1 h red light irradiation) then stained with DCFH-DA for 30 min at 37°C. Statistical significance was determined relative to the treatment with conjugates alone and indicated by \*p < 0.05, \*\*p < 0.01, and \*\*\*p < 0.001 using one-way ANOVA. Data represented as mean ± SD (n = 2 replicates).

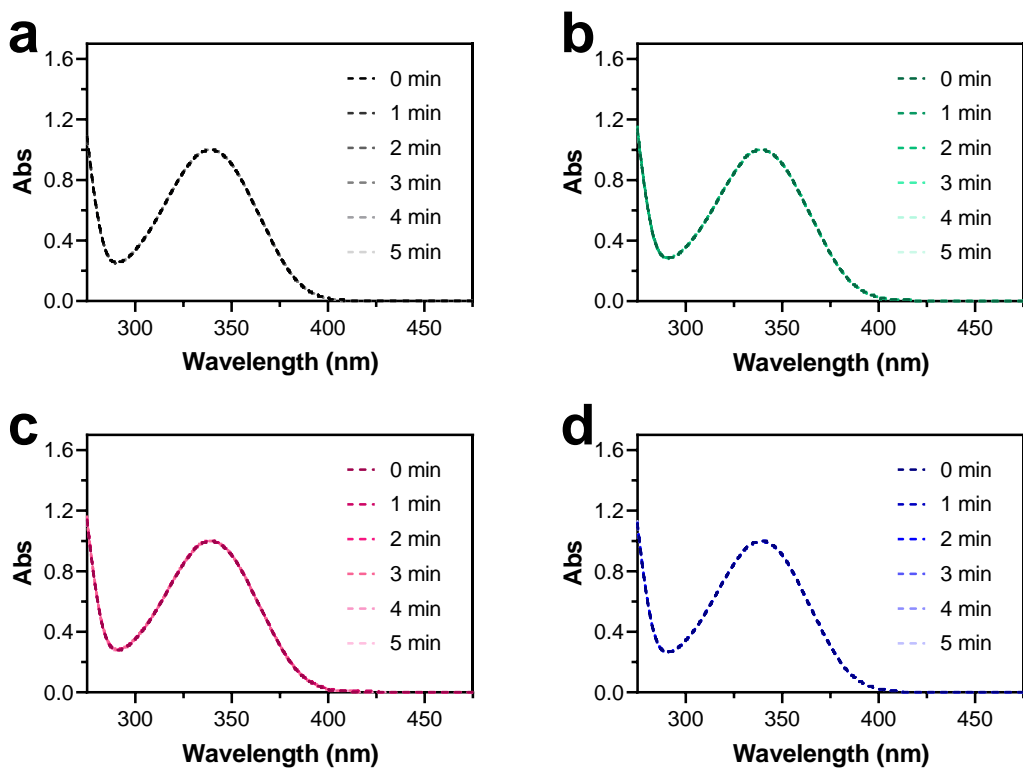


**Figure S25.** Absence of NADH (160 mM) oxidation in PBS in the absence (a) and in the presence of Ir(III)-COUPY conjugates **3a** (b), **3b** (c) and **3c** (d) (10  $\mu$ M) in the dark.

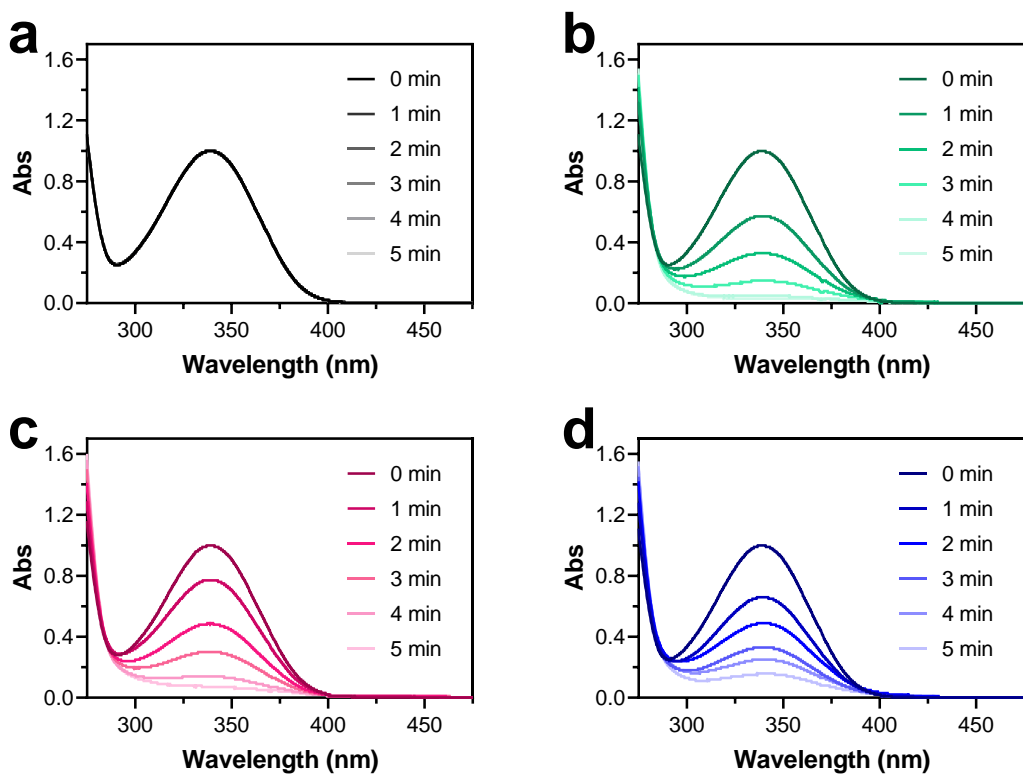


**Figure S26.** Photocatalytic oxidation of NADH (160 mM) in PBS in the absence (a) and in the presence of Ir(III)-COUPY conjugates **3a** (b), **3b** (c) and **3c** (d) (10  $\mu$ M) upon irradiation with red light ( $620\pm15$  nm; 130 mW  $\text{cm}^{-2}$ ).

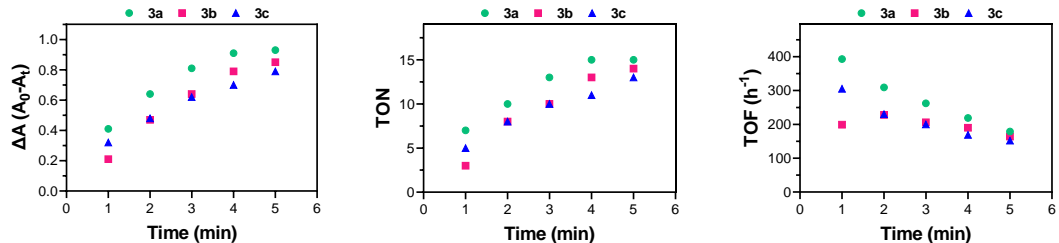
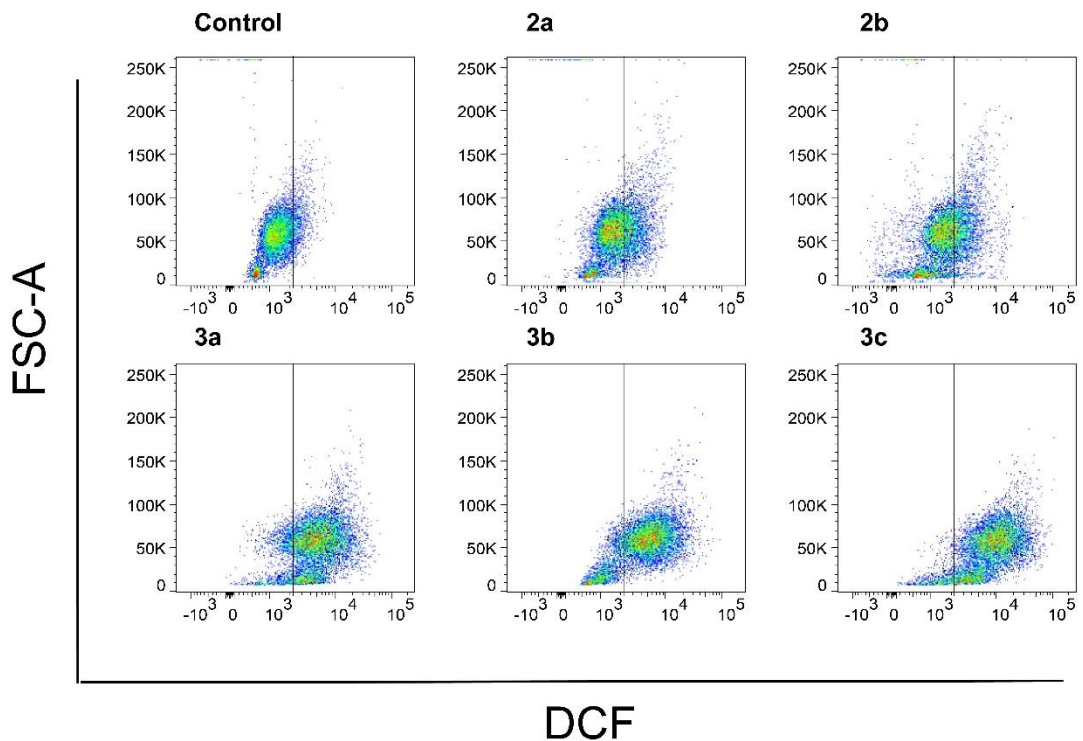


**Figure S27.** Determination of the catalytic efficiency of Ir(III)-COUPY conjugates **3a**-**3c** (10  $\mu$ M) in the photooxidation of NADH (160  $\mu$ M) in PBS upon irradiation with red light ( $620\pm15$  nm; 130 mW  $\text{cm}^{-2}$ ). Acronyms: turnover number (TON), turnover frequency (TOF).



**DCF**

**Figure S28.** ROS generation in A2780cis cells under hypoxia after PDT treatment with the investigated compounds as detected by flow cytometry in FL1-H channel upon DCFH-DA staining (DCF fluorescence plot) vs. cell size (FSC-A). Non-treated, irradiated cells served as a control. A region line was used to gate cell populations with high vs. low DCF fluorescence. Light irradiation condition: 620 nm light, 90 mW/cm<sup>2</sup>, 1 h.

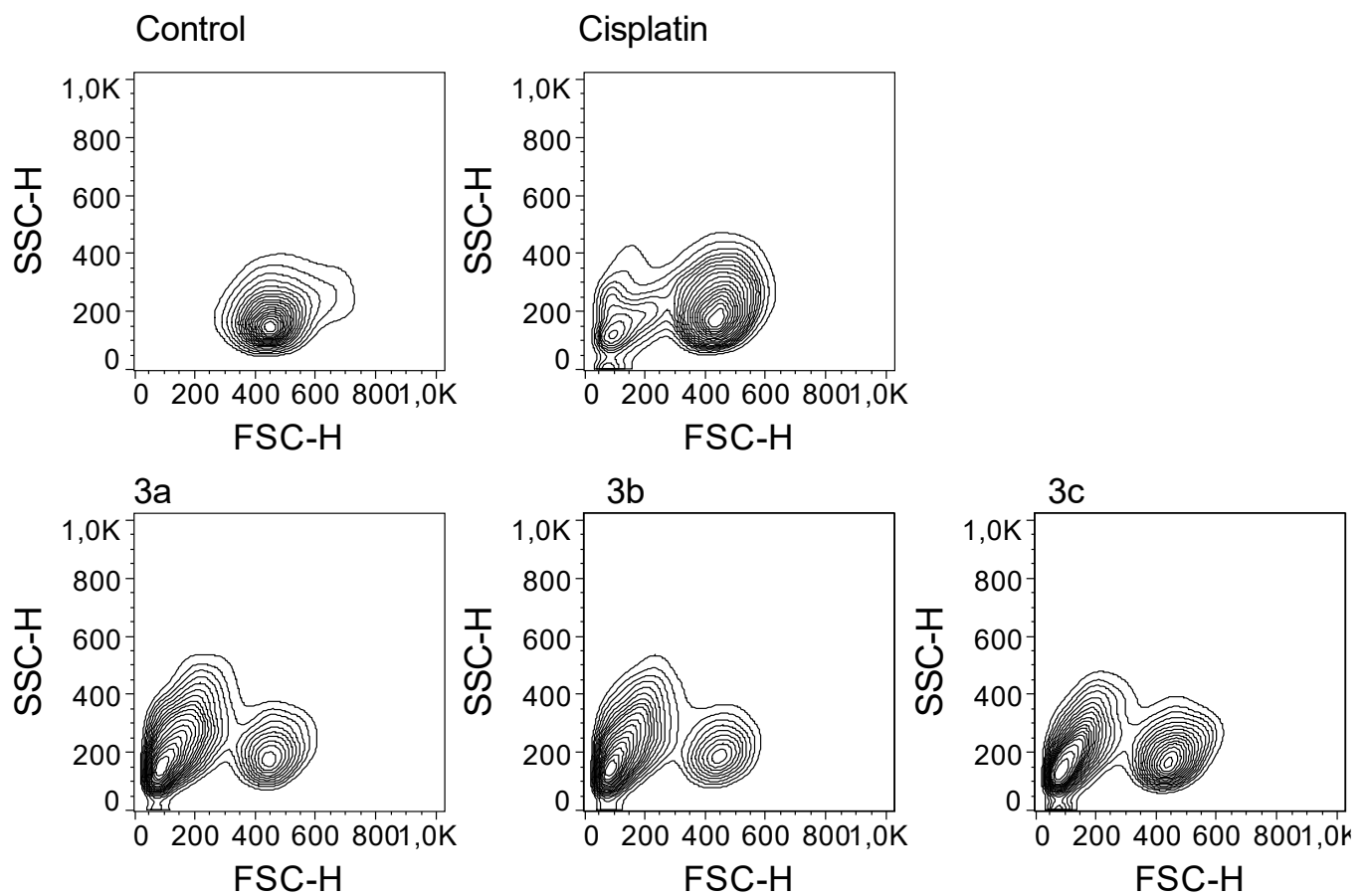
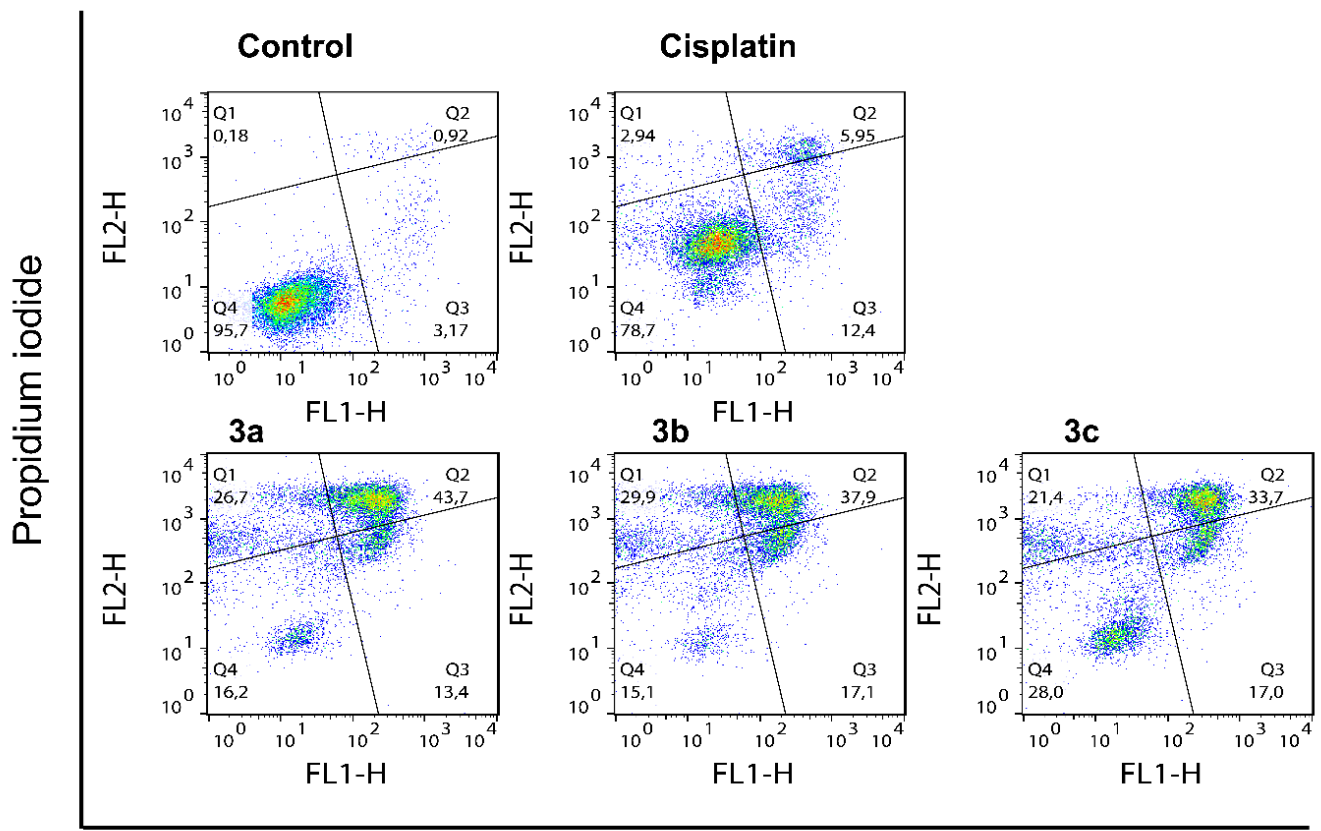
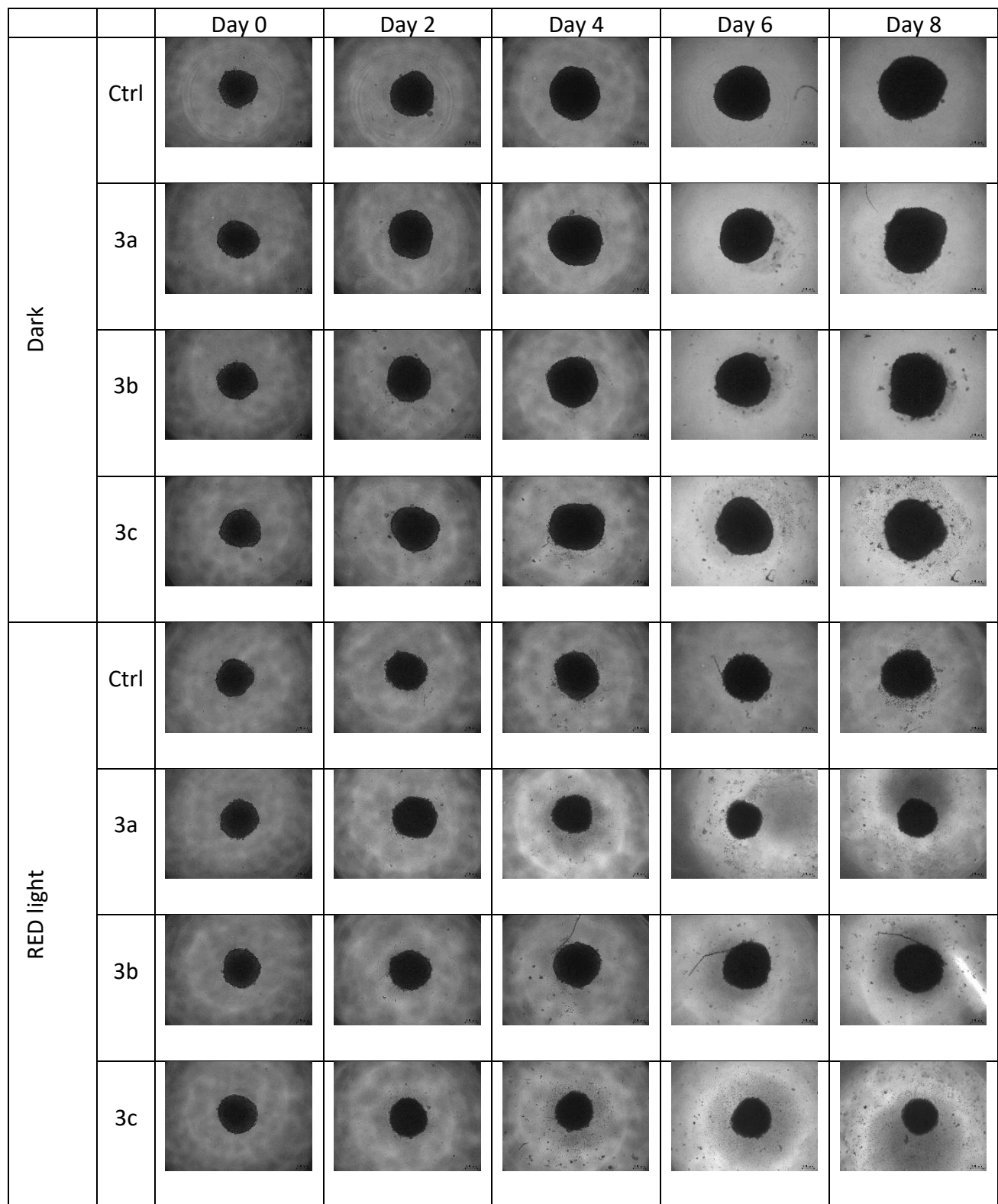


**Figure S29.** Representative cell size (FSC-H) vs. cell complexity (SSC-H) contour plots of A2780cis cells after PDT treatments with Ir(III)-COUPY conjugates ( $10 \mu\text{M}$ , 1 h). Light irradiation condition: 620 nm light,  $90 \text{ mW/cm}^2$ , 1 h.

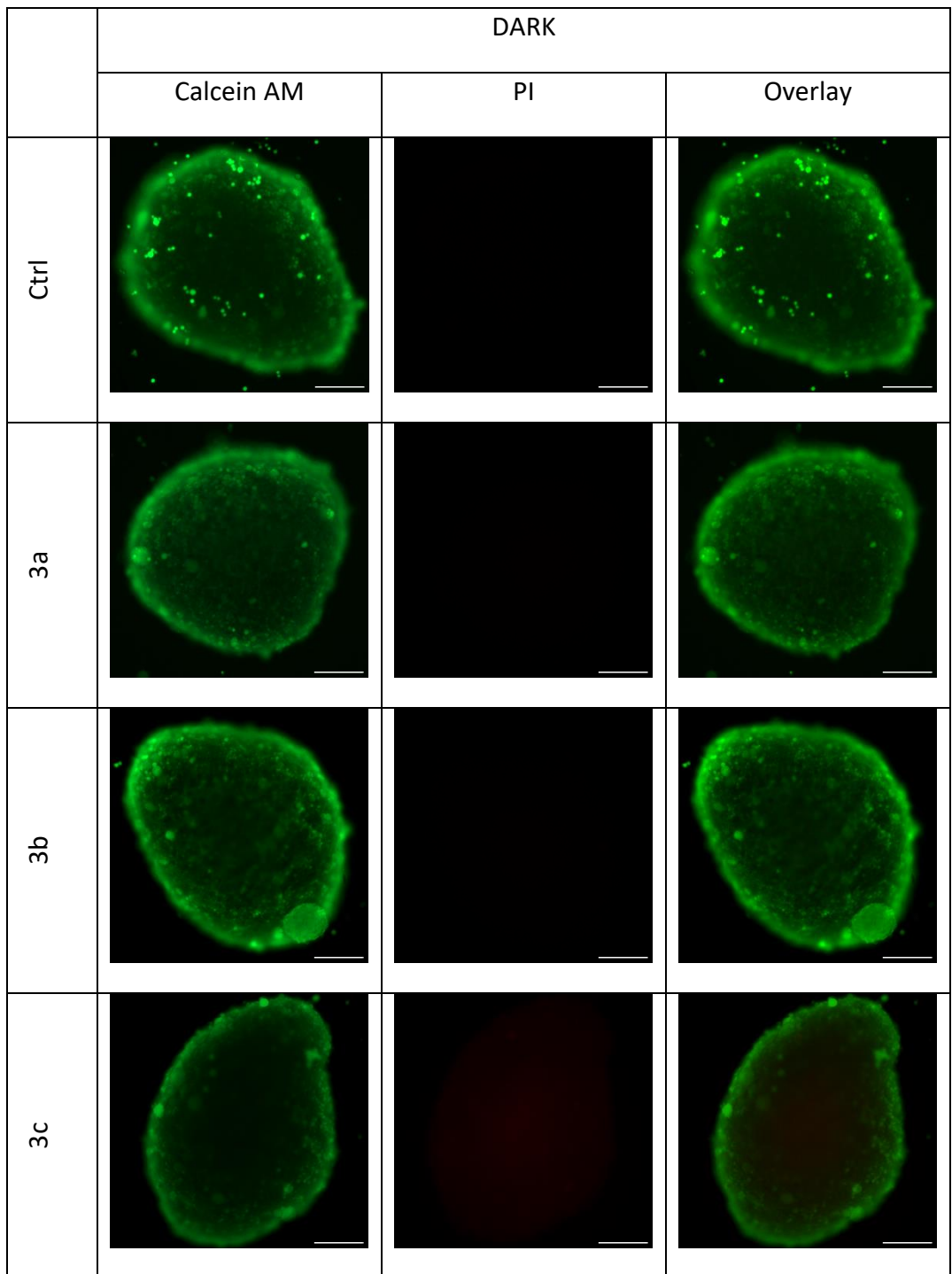


### Annexin V-FITC

**Figure S30.** Representative double-stained Annexin V-FITC (FL1)/Propidium iodide (FL2) dot plots of A2780cis cells after PDT treatments with Ir(III)-COUPY conjugates (10  $\mu$ M, 1 h). Light irradiation condition: 620 nm light, 90 mW/cm<sup>2</sup>, 1 h.



**Figure S31.** Alterations in EO771-derived MCTS observed over 8 days after treatment with 20  $\mu$ M of **3a**, **3b** and **3c**, followed by 1-hour red light irradiation. The control was kept in both dark and light conditions. Scale bar: 200  $\mu$ m.



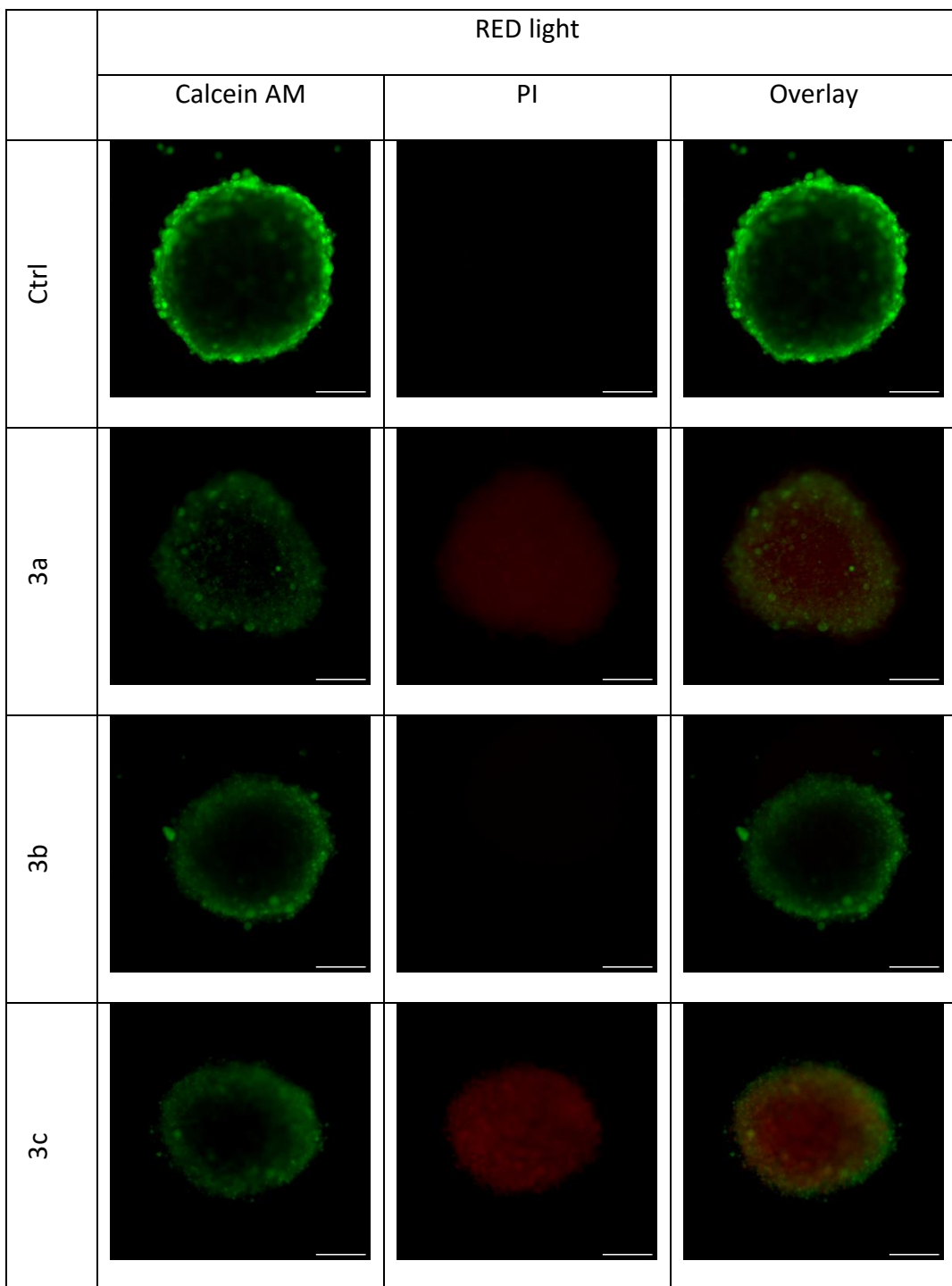


**Figure 32.** Analysis of the EO771 spheroids using fluorescence microscopy. MCTS were treated with **3a**, **3b** and **3c** (20  $\mu$ M) for 1 hours, followed by 1-hour red light irradiation and observation after 4 days of incubation, with an additional treatment after the second day. Spheroids were stained with Calcein AM (2  $\mu$ M) and propidium iodide (2  $\mu$ g/mL). The same treatments were kept in dark conditions as a control. The scale bar represents 200  $\mu$ m.

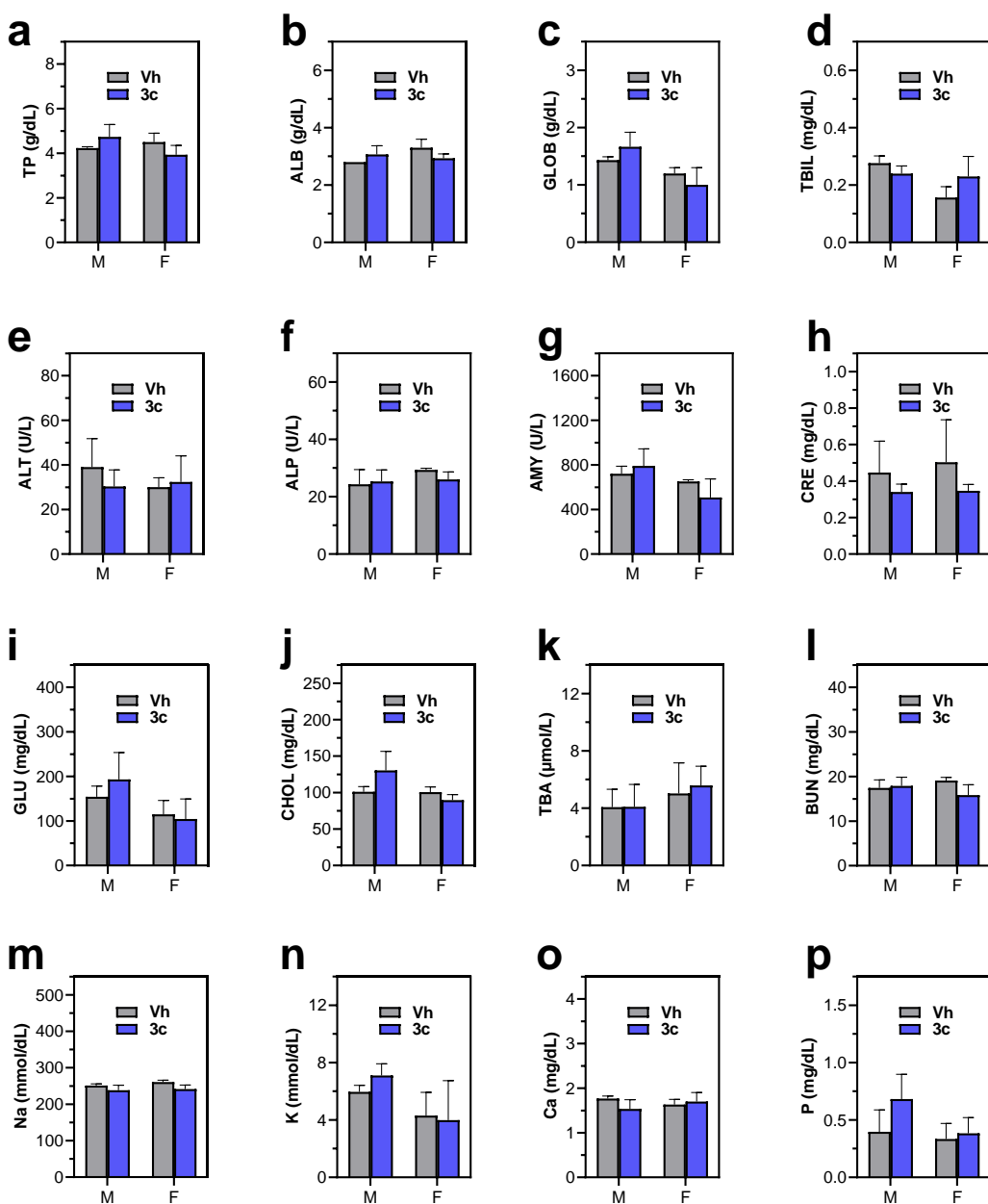


**Figure S33.** Plasma biochemistry analysis of C57BL6/Hsd mice following an acute intraperitoneal injection of compound **3c** (5 mg/kg) compared to a vehicle (Vh) control. Mice were sacrificed 7 days post-treatment. Notes (a-p): the following parameters were assessed in both male (M) and female (F) mice (n=3 per group): total proteins (TP), albumin (ALB), globulins (GLOB), total bilirubin (TBIL), alanine aminotransferase (ALT), alkaline phosphatase (ALP), amylase (AMY), creatinine (CRE), glucose (GLU), cholesterol (CHOL), total bile acids (TBA), blood urea nitrogen (BUN), sodium (Na), potassium (K), calcium (Ca), and phosphorus (P). Values are presented as the mean  $\pm$  standard deviation.





H	-1.356275	-6.164521	-6.526842
H	4.083354	0.697226	-1.105721
H	6.138962	1.738734	-0.796572
H	6.951761	0.341375	-1.518881
H	6.079473	1.026894	-3.770233
H	5.397949	2.491118	-3.054675
H	7.675430	3.244042	-2.394187
H	8.370546	1.764616	-3.022897
H	7.557381	2.368665	-5.236942
H	9.100838	5.825389	-4.266336
H	7.461057	6.313492	-4.641989
H	5.703867	5.780886	-3.113826
H	5.052027	5.798361	-0.767463
H	9.247082	5.352085	0.234457
H	6.297987	5.398992	4.087390
H	1.446122	5.375104	4.647485
H	-0.370443	5.419570	3.059637
H	2.488603	5.879443	-0.174389
H	1.103554	4.961814	-1.217685
H	-0.603779	4.771491	-1.483704
H	0.287420	6.687153	-2.801537
H	-0.905969	7.256559	-1.630127
H	0.822337	7.492539	-1.314771
H	-2.069744	5.010202	-0.041116
H	-1.595675	4.638406	1.597726
H	-3.159546	6.569468	1.547796
H	-1.583098	7.141271	2.118330
H	-2.084323	7.453377	0.450782
H	4.962323	5.295032	6.011651
H	3.425425	6.176731	5.910690
H	3.437904	4.420478	5.764541
H	-4.721201	1.635002	2.942198
H	-4.561496	3.012908	1.881279
H	-5.318716	-0.514062	0.851631
H	-7.397028	-1.190578	-0.281286
H	-8.957578	2.781906	0.187369
H	-6.891487	3.453119	1.365895
H	3.369532	1.697022	-4.695558
H	2.926879	1.729745	-6.382701
H	1.292029	4.483007	-4.677921
H	2.109797	6.815266	-4.696866
H	5.831254	5.491502	-6.403875
H	5.030142	3.173897	-6.352191
H	9.725111	5.363197	-2.169550